ANNUAL REPORT

COMBUSTION OF AMMONIUM PERCHLORATE-POLYMER SANDWICHES

By

E. W. Price, J. K. Sambamurthi,
R. R. Panyam and R.K. Sigman

Prepared for

OFFICE OF NAVAL RESEARCH
800 North Quincy Street
Arlington, Virginia 22217

Under

Contract N00014-79-C-0764; NR 092-566

FEBRUARY 1984

GEORGIA INSTITUTE OF TECHNOLOGY
A UNIT OF THE UNIVERSITY SYSTEM OF GEORGIA
SCHOOL OF AEROSPACE ENGINEERING
ATLANTA, GEORGIA 30332

1984

Unclassified

SECURITY CLASSIFICATION OF THIS PAGE (When Data Entered)

REPORT DOCUMENTATION PAGE		READ INSTRUCTIONS BEFORE COMPLETING FORM
1. REPORT NUMBER	2. GOVT ACCESSION NO. AD-A139 873	3. RECIPIENT'S CATALOG NUMBER
4. TITLE (and Subtitle) Combustion of Ammonium Perchlorate-Polymer Sandwiches		5. TYPE OF REPORT & PERIOD COVERED Annual Report Aug. 1982 - Oct. 1983
		6. PERFORMING ORG. REPORT NUMBER
7. AUTHOR(s) Edward W. Price, Jayaraman K. Sambamurthi, Ramaprasad R. Panyam and Robert K. Sigman		8. CONTRACT OR GRANT NUMBER(s) ONR Contract No. N00014-79-C-0764
9. PERFORMING ORGANIZATION NAME AND ADDRESS School of Aerospace Engineering Georgia Institute of Technology Atlanta, Georgia 30332		10. PROGRAM ELEMENT, PROJECT, TASK AREA & WORK UNIT NUMBERS
11. CONTROLLING OFFICE NAME AND ADDRESS Mechanics Division, Office of Naval Research Department of the Navy, 800 N. Quincy Street Arlington, Virginia 22212		12. REPORT DATE February 1984
		13. NUMBER OF PAGES 73
14. MONITORING AGENCY NAME & ADDRESS(if different from Controlling Office)		15. SECURITY CLASS. (of this report) Unclassified
		15a. DECLASSIFICATION/DOWNGRADING SCHEDULE

16. DISTRIBUTION STATEMENT (of this Report)

Approved for public release; distribution unlimited.

17. DISTRIBUTION STATEMENT (of the abstract entered in Block 20, if different from Report)

Approved for public release; distribution unlimited.

18. SUPPLEMENTARY NOTES

19. KEY WORDS (Continue on reverse side if necessary and identify by block number)

Combustion, Solid Propellants, Rockets, Ammonium Perchlorate, Flames

20. ABSTRACT (Continue on reverse side if necessary and identify by block number)

A summary of results of experimental studies of combustion of AP-polymer sandwiches is reported. Most recent results are combined with those of a previous report, and mechanistic interpretations are presented. On the basis of these interpretations, a detailed qualitative model of the combustion zone structure is advanced, and examined for consistency with results of this and other studies. The results are tested by prediction of a singular feature of the

DD FORM 1 JAN 73 1473 EDITION OF 1 NOV 65 IS OBSOLETE

Unclassified

SECURITY CLASSIFICATION OF THIS PAGE (When Data Entered)

burning of propellants, and propellant tests are reported that confirm the predictions. The results indicate that the combustion of AP-hydrocarbon binder propellants involves closely coupled, three-dimensional interactions among several regions of the flame complex. These features are important to understanding both steady state and oscillatory combustion.

Acknowledgements

This research has been sponsored by the Mechanics Division of the Office of Naval Research, Arlington, Virginia, under Contract No. N00014-79-C-0764. The authors wish to express their appreciation for the thoughtful and patient monitorship of Dr. R. S. Miller, and for the continuity of support so vital to progress in this multifaceted problem.

Table of Contents

Introduction

The combustion of composite solid rocket propellants takes place in a thin region close to the surface of the propellant. The thickness of this region is dictated by the necessity to transfer heat back to the solid at a rate sufficient to maintain the rate of pyrolysis at the surface required in applications of the propellant. This in turn dictates that the scale of heterogeniety (usually set by oxidizer particle size) be small enough for fuel and oxidizer vapors to mix in the thin region near the surface. In practice, the dimensional scale turns out to be of order 100 μm, a scale encompassing an intricate flame complex (e.g., Ref. 1). Experimental observation on such a dimensional scale is virtually impossible, a circumstance that has led to a rather speculative quality of research and literature on combustion mechanisms. The situation is further complicated by the uncertain relevance of flame theory when applied to such small, geometrically and chemically complicated flame systems.

A strategy to alleviate some of the experimental difficulties of observation is to study combustion of geometrically simple systems such as the oxidizer-binder sandwich. By edge burning these laminate structures, the combustion zone often conforms to a two-dimensional steady state configuration, hopefully amenable to more meaningful observation and theoretical interpretation. If this goal is achieved, then at least some aspects of the more complex propellant combustion problem can be clarified. Unfortunately, the micro-combustion zone is still substantially inaccessible to experimental observation, even in the

geometrically simple systems, so the strategies for research are still less direct than would be desired, and results correspondingly more speculative. One exception to the limitations of spatial resolution in measurements is the quench-burning experiments, which permit leisurely study of the surface of a quenched sample under high magnification (Fig. 1). Such experiments typically interrupt burning very abruptly by rapid depressurization of the combustor. While some artifacts are produced by the quench event, the details of the burning surface microstructure are largely preserved and can be used in combination with other information to infer combustion zone structure.

The sandwich approach has been used by many investigators (e.g., Powling,[2] Hightower and Price,[3,4] Boggs et al.,[5] Netzer et al.,[6,7] Nadaud,[8] Ermolaev et al.[9]). It has become evident in recent work[10,11] that relevance to propellant combustion requires that binder laminae in sandwiches be very thin (to avoid anomalous effects such as binder melt flow that would not occur with high solids AP-HC binder propellants). It is also important that interpretation of results address observations near enough to the oxidizer-binder interfaces to correspond to situations possible on propellant surfaces (where the surfaces of exposed oxidizer particles are typically 100 μm across). In hindsight, these considerations may seem obvious, but a significant amount of published work on sandwiches of propellant ingredients has addressed either situations or aspects of results that were only marginally relevant to conventional propellants. The present studies, involving sandwiches of ammonium perchlorate and typical

hydrocarbon binders, used primarily sandwiches with binder laminae of 10 - 100 μm thickness.

Earlier tests[3,5,10,11] had shown certain critical features of quenched thin binder sandwiches of interest, which are summarized here so they can be used in interpretation of results:

1. The larger features of surface profiles are shown in Fig. 2 (See Ref. 10-12).

2. The details in the vicinity of the binder lamina are shown in Fig. 3. Part a shows the trend with binder thickness. Part b shows the trend with pressure (for a binder thickness of 50 - 70 μm). Fig. 1 shows certain features of surface quality that are persistent in varying degree for all tested conditions on AP-hydrocarbon binder sandwiches with thin binder laminae, described further below (See Ref. 3-5, 10-17).

3. All test samples from tests above 2 MPa exhibited regions of the AP surface ("distant" from the binder lamina) with the characteristic surface qualities of AP self-deflagration (Fig. 1), including flaky residue of a surface melt layer, and larger scale surface patterns of ridges and depressions (e.g., Ref. 3-5, 10-19).

4. All thin-binder test samples showed (Fig. 3a,b) the binder lamina to be recessed relative to the region of the oxidizer laminae immediately adjoining the binder[3-5, 10-12] (binder lamina thickness less than 40 μm).

5. All test samples showed a region of the AP lamina centered 25 - 75 μm out from the binder interface plane that was the leading edge of the AP surface regression, i.e., the AP closer to the binder protruded[10-12] (Fig. 1, 3).

6. The surface of the AP in the protruding region adjoining the binder showed a distinctive, relatively smooth quality, with no flake relic of the AP melt (Fig. 1). This "smooth band" adjoining the oxidizer-binder interface was evident even with a binder (polysulfide) that pyrolized without evidence of a melt state,[10-12] suggesting that the smooth surface is not due to the binder melt flows commonly observed in thick-binder sandwiches.[3,5,6,16,17]

The present studies pursue the investigation of sandwich burning in further detail, with the goal of establishing a correct description of the flame complex. It is re-emphasized that direct measurements of the flame are precluded by the "smallness" and complexity of the reaction region. A correct description depends on a process of inference from systematic observations of global combustion behavior (e.g., burning rate); measurable combustion zone microstructure (quenched samples); independent information about ingredient decomposition and combustion; and basic flame theory. In the following, several new investigations of sandwich burning are described, and the results are combined with the above sources of information and the previous results summarized in 1 - 6 above. The result is a relatively detailed description of the combustion zone. In the interest of brevity, the experiments and results of the present studies are first summarized below with a minimum of discussion, and with frequent reference to other sources for details.

Experimental Procedure

The investigations will be described in sequence in very briet torm. This will be followed by descriptions of preparation ot test samples and test procedure.

The Experiments

1. Interrupted burning tests on sandwiches with laminae ot unitorm thickness, to determine the nature ot the burning surtace.[10-12,15] In these tests, the samples were quenched by rapid depressurization and the burned surtaces were examined in a scanning electron microscope. The test variables were test pressure, polymer lamina thickness, and substitution ot other materials for the polymers (e.g., mica, gold, and a blend ot polymer and tine ammonium perchlorate powder). The ettect ot these variables on the burning surtace protile and surtace quality provide indirect evidence ot what is happening to the tlame structure.

2. Burning rate ot sandwiches as a tunction ot binder thickness and pressure.[18] In these tests, PBAN laminae ot particulaly unitorm thickness were used, and burning rate was measured by combustion photography.

3. Detlagration limits ot AP-polymer sandwiches.[10,11,15,20,21] Constant pressure tests were run on sandwiches with "tapered" polymer laminae. Samples were ignited along the thick-binder edges ot the sandwiches, and burning proceeded with progressive decrease in binder thickness. At test pressures below the AP selt-d tlagration limit, the samples spontaneously quenched before comp.... bu.. iout, and the thickness ot the binder at the quench surtace was measured in the SEM. Tests were run over the pressure range 0.1 to 2.4 MPa,

with HTPB, PBAN and polysulfide binder.

4. Effect of oxidizer particle size on propellant burning rate. A family of propellants was prepared and burning rate determined over a pressure range. The propellants were formulated to test the relevance of a "sandwich-based" concept (regarding combustion zone structure) to the propellant burning situation. The propellants used bimodal oxizider particle size distribution, with the size of the fine component being nominally 18, 49 and 82 μm. Burning rates were determined by combustion photography.

Test Samples

Sandwich samples were prepared by methods and to sizes described previously.[10,15,18] Ammonium perchlorate laminae were prepared from Kerr-McGee high purity AP (nominal 100 μm particles). The powder was pressed at 210 MPa for a minimum of 20 minutes in a stainless steel die, yielding laminae 1.3 mm thick. Most sandwiches were made by bonding two laminae together with the polymeric binder. Thickness of the binder was controlled with spacer shims. Two types of polymer sandwiches were used. Plane-parallel laminae were used on burning rate tests and depressurization quench tests. "Tapered" polymer laminae[10,11,15,21] used in spontaneous quench tests were prepared by using a spacer shim in one edge of the laminate only. Light pressure during curing resulted in the thin edge of the binder lamina of such samples being less than 10 μm thick.

In order to assure that no extraneous combustion effects would result from unsuspected characteristics of the pressed AP laminae, their self deflagration was compared with that of single crystal samples. The quenched surface characteristics were similar to those of single crystals, except for somewhat

greater irregularity in surface pattern. Burning rates were the same as reported by Boggs for single crystals.[14,19] Samples were prepared with different AP particle size, and with reduced compaction pressures (131 and 61 MPa), and used in quench-burning tests on sandwiches. No effect was evident in the characteristics or profiles of quenched surfaces. Some concern that fuel species might migrate into the surface layers of the AP laminae before testing was allayed by these results.

Sandwich samples were also made in which the binder (fuel) lamina was either omitted or replaced by a sheet of mica or gold.[20,21] The objective was to clarify the mechanistic effects of the binder lamina. Efforts to dry-press these "binderless" sandwiches to assure good thermal and physical contact between laminae were unsuccessful, so the dry sandwich laminae were held together during tests by light pressure from a metal clip. While the test results suggest that contact between laminae was not perfectly uniform, burning behavior was fairly regular.

Sandwich samples were also made in which the fuel lamina was a mixture of binder and 10 μm AP.[20,21] These were plane-parallel samples for use in depressurization quench tests. Samples were made with several "binder" laminae thicknesses, and in AP-binder mix mass ratios of 1:1 and 7:3. The mix was prepared by hand stirring for 20 minutes, followed by settling in a vacuum for 15 minutes to remove air bubbles. Sandwiches were then prepared in the same way as with pure binder laminae. Table I shows the binder thickness-mix mass ratios actually tested.

The experiments with bimodal propellant samples called for a series of formulations in which a relatively coarse fraction of AP (400 μm) was combined with a relatively fine fraction (i.e., bimodal AP size distribution). The series of propellants called for a graduated sequence of particle sizes of the fine

component of the AP. For the intended purpose it was desirable to have a narrow size distribution within each size mode, and it was judged that the fine component mean sizes should be in the range 20-100 μm (see Discussion). These specifications were not fully achievable from available resources; accordingly, propellants were prepared with less ideal specifications as described in the following. Commercial high purity AP was available in a nominal size of 400 μm. This material was screened to limit its size variability to a range of 425 μm to 335 μm. Finer components were prepared in nominal sizes of 17.5, 49.0 and 82.5 μm by screening ground high purity AP. These nominal size designations are simply the mid-points of the size ranges, established by the screen mesh sizes used, which were 37 mesh pass for nominal 17.5 μm; 45 and 53 mesh for nominal 49.0 μm; and 75 and 90 mesh for nominal 82.5 μm. No attempt was made to quantity the size distributions within these sized samples, because the objective of the experiment required only demonstration of a specific qualitative difference in burning rate behavior of the propellants. The propellants were prepared by hand-mixing 4 gm batches in an open beaker. The AP, monomer and curing agent were measured in amounts that yielded 71% 400 μm AP, 16.5% fine component AP, and 12.5% PBAN binder. After 15 minutes of mixing, the mixture was placed under vacuum at room temperature for 30 minutes. The mixture was then transferred to rectangular molds of dimensions 30 mms x 12 mms x 2.5 mms and hand pressed by tapping the mixture for 20-30 minutes with a 1 cm diameter cylindrical teflon stick. The samples were then cured in an oven at 72°C for 7 days. The cured propellants were cut into rectangular samples (10 mm x 6 mm x 2.0 mm) for burning rate tests.

Test Procedures

Experimental methods in the present work are mostly routine and reported elsewhere.[10-12,15,18,20,21] Sandwich samples were nominally 10 x 6 x 2.8 mm;

they were mounted on a pedestal in a nitrogen-filled high pressure vessel and ignited on the top (6 x 2.8 mm) edge by an electrically heated wire. Propellant samples were 10 x 6 x 1.6 mm, mounted and ignited in a similar manner to the sandwiches. For combustion photography, a flushed windowed pressure vessel was used, with illumination of the sample from outside. For quench tests, a non-flushed pressure vessel was used that is equipped with pressure-release burst diaphragms. Characterization of samples after tests (quench tests) consisted primarily of surface quality, surface profile, and dimensional details as revealed in the scanning electron microscope. The thickness of the binder lamina of quenched samples, as reported in the Results, was measured in the SEM. In all tests on plane parallel sandwiches where the lamina thickness of the entire sample was needed, the edges of the sample were examined before the test in an optical microscope or SEM to provide an estimate of average thickness and to disqualify samples with nonuniform thickness. This was particularly important in tests on burning rate, because rate is sensitive to thickness and there is no quenched sandwich to measure after the test. Variation of edge thicknesses of a binder laminae of more than $\pm$ 5 μm disqualified samples for burning rate tests; with care in sample preparation, this led to a rejection rate of about 50%.

Burning rates of both sandwiches and propellant samples were measured by projection of the motion pictures and measurement of timing marks and burning surface recession. This permitted any instances of uneven burning to be recognized and excluded from the rate data. Thirty percent of all tests were run in duplicate to monitor reproducibility; the test conditions for duplicate tests were selected randomly before any testing. For duplicate samples that burned evenly, no significant differences in rate were obtained. Most samples burned evenly.

Results

The experimental results are summarized in the following; because several separate investigations are covered, results of each investigation are accompanied by some interpretation as needed to explain why the tests were run. Then in a subsequent section, the interpretations are enlarged and combined to provide a qualitative description of the processes of sandwich burning.

Surface Profiles and Burning Surface-Binder Substitutes

The persistence of the smooth band and protrusion of AP at the AP-binder interfaces was noted in earlier work and in the Introduction (Fig. 1,3), and observed also in the present work. This effect was attributed in an earlier report[20,21] to the effect of lateral heat flow from the oxidizer to the endothermic binder. Tests with other materials substituted for the binder were run to test this postulate. The choice of mica was made because it is a non-burning material with low thermal conductivity. The choice of gold was made because it is a non-burning material with high thermal conductivity. Presumably, the effect of lateral heat flow would remain with a gold lamina, and would be absent with a mica lamina. The tests with two AP laminae in direct contact were run as a control to test the effect of dry contact with no intervening lamina. The test results are typified by the examples in Fig. 4. Part a is from a control test with a 100 μm thick lamina of PBAN. Part b shows the details of the sandwich surface from a 4.2 MPa test on a sandwich with a mica lamina in place of the binder (the right side of the picture is the somewhat delaminated side of the protruding mica lamina; the AP surface on the left is in the region normally occupied by the smooth band). The detail shown in this figure is typical of the

interface region in these "mica" tests. It is also typical of the self-deflagration of AP, normally exhibited on the AP laminae of sandwiches only at surface sites further from the interface. With mica laminae there was no smooth band and no protrusion of AP in the interface region.

Part c of Fig. 4 shows the quenched surface of a sample consisting simply of two AP laminae held together during burning by a metal clip. The figure shows the characteristics of simple AP deflagration, uninterrupted up to the interface plane. Under high magnification it was evident that the surfaces of the two slabs were together during burning; surface patterns near adjoining edges are correlated, and the edges show some matched features indicative of separation of a contiguous surface layer that is liquid during burning. There is no protrusion of the AP laminae in the interface region. Separation of the two laminae, visible in the example, occurs during handling after the test.

Part d of Fig. 4 shows the quenched surface of an AP sandwich in which the binder lamina was replaced by a 15 μm layer of gold. Such samples consistently showed retarded burning (protruding AP) in the vicinity of the gold lamina, and a relatively smooth surface there. This behavior was not as uniform along the lamina as with a binder lamina, but was predominant. The nonuniformity is attributed to the difficulty in achieving uniform thermal contact between dry laminae. It is stressed that the "smooth band" phenomenon described here is not a manifestation of the binder melt flow reported in many earlier studies. With thin-binder sandwiches used in the present studies, melt flow is minimal,[10-12,15] and available results show that the smooth band is present even with a non-melting polysulfide binder[10] and with the gold lamina. The combined results are very strong evidence that the smooth band and protruding AP near the contact planes of conventional thin-binder sandwiches are caused by lateral heat flow into the binder lamina, with some corresponding modification of the AP

decomposition-deflagration in the smooth band region. This conclusion is in contrast to that of Boggs[5], and of the present authors in early reports[15], who attributed smooth bands to binder melt flow (most investigators agree on the presence of melt flow with thick binder laminae; most investigators have not done extensive testing with thin binder laminae).

In addition to the above tests designed specifically to explore the cause of the smooth band and AP protrusion adjoining the contact surfaces, many other tests are reported here that were run for other purposes. In all cases where a pure binder lamina was used, the features 1 - 6 of the profiles and quenched surfaces as described in the Introduction were evident in a manner consistent with the trends described here.

Burning Rate of Sandwiches

The results of the sandwich burning rate tests[18] are shown in Fig. 5a. At large binder thickness the rate appears to approach a limit at each pressure (the limit is of only peripheral interest in the present study). As binder thickness is reduced, the burning rate increases to a maximum at a thickness of 65-85 μm, and then decreases for thinner binder. At pressures above the AP self-deflagration limit, the AP rate is approached as the binder thickness goes to zero. At lower pressure, decreasing binder thickness leads to a quench limit (measured in the "tapered" sandwich tests; see broken curve, lower left, Fig. 5a). The enhancement in burning rate by the binder lamina is strongest in the intermediate pressure range. Under conditions of rate enhancement (over the AP rate), the combustion front burns down the sample and leaves a trailing oxidizer profile that is "V"-shaped (Fig. 2e) when the test is above the AP self-deflagration limit, and "U"-shaped (Fig. 2d) below the AP self-deflagration limit. It was noted earlier[10-12,15,20,21] and in Fig. 2c,f that at higher pressures the AP

self deflagration leads the sandwich burning front, so it may be concluded that the family of curves in Fig. 5a would consist of horizontal lines at pressures much higher than reported in the figure. A partial cross plot of the curves in Fig. 5a as burning rate vs pressure is shown in Fig. 5b. This figure shows the AP self-deflagration rate (lower curve); the conditions for maximum sandwich rate (top curve); and the "thick slab limit," i.e., asymptotic rate for thick binder (middle curve). By extrapolation of the curve of maximum sandwich rate, the enhancement in rate over the AP rate is seen to go to zero around 7 MPa. The thick slab rate is seen to approach the AP rate at about 3 MPa. In summary,

1. AP does not burn below 2 MPa, but sandwiches burn down to about atmospheric pressure unless the binder is too thin.
2. Between 2 MPa and 7 MPa, thin-binder sandwiches burn faster than AP alone.
3. Above 7 MPa, all sandwiches burn at the self-deflagration rate of AP.

These limits may differ with different binders. The trend in 3 probably does not apply to pressures above 14 MPa, where a transition in AP behavior occurs.[14,22]

Deflagration Limit

Results of the spontaneous quench tests on tapered sandwiches are summarized in Fig. 6 for three binder materials.[10,11,20,21] The error bars on the data points represent the range of variation of thickness of the binder lamina along the quenched edge, as measured in the SEM. Over the pressure range of 0.4 - 2.0 MPa, the sandwiches with any particular binder tended to quench at roughly the same binder thickness. Above 2.0 MPa, samples usually burned to

completion, a result that is consistent with the fact that AP self-deflagrates above 2.0 MPa. At pressures below 0.4 MPa, the binder thickness for self quenching became increasingly pressure dependent. Limited testing was made with samples with different degrees of taper of the binder lamina to test the possibility that the quench limit might be dependent on details of the approach to the limit. No statistically significant effect was evident. The different binders yielded significantly different quench limits in the 0.4 - 2.0 MPa range. Figure 7 shows a scanning electron microscope picture of a typical spontaneously quenched sample. The general features are similar to those of samples with binder lamina of uniform thickness quenched by rapid depressurization from comparable pressures. This indicates that approach of the tapered sandwich to self quench does not involve development of any singular features of surface configuration. The thickness measurements in Fig. 6 were obtained from SEM pictures similar to Fig. 7, with suitable magnification.

AP-Filled Binder Lamina Sandwiches

Test conditions are summarized in Table I. Results of tests are summarized in Fig. 8 - 10. Figure 8 shows a comparison of quenched sandwiches with pure binder and with 1:1 AP-filled binder.[20,21] From these tests (6.9 MPa, nominal lamina thickness 70 μm) there is an obvious difference between behavior of sandwiches with and without AP in the binder. From extensive examination of samples with 1:1 laminae, it was evident that the region of protruding AP is widened and protrudes less with AP-filled laminae. The protruding region is flat on top, and the surface quality is smooth. The binder lamina is recessed and the surface of that lamina shows undulations of the same dimensional scale as the AP

filler. However, no distinguishable AP particle surface is evident there. The details conform qualitatively to the general features 1 - 6 noted in the Introduction, but differ unambiguously from those of sandwiches with pure binder laminae in the details noted above. The differences become less evident at lower pressures.

Use of a higher mass ratio of AP to binder (7:3) in the "binder" lamina resulted in more conspicuous deviation from the results with pure binder laminae. The basic difference is illustrated for 6.9 MPa in Fig. 9 (upper right), which shows regions of both AP and binder adjacent to the AP-binder interface planes that are recessed relative to the protruding AP.

The comparison in Fig. 9 is for samples with filled binder laminae that are about 70 μm thick. With 1:1 AP-binder laminae, the profiles were not critically dependent on lamina thickness. However, for the 7:3 laminae it was found that the profile was highly dependent on lamina thickness (6.9 MPa) as shown in Fig. 10. With very thin laminae, the profile was similar to that with 1:1 mixture. As lamina thickness increased, the lamina region became increasingly recessed, and the overall sample profile became "V"-shaped (a configuration indicating that the lamina-interface region is dominating the sandwich burning rate). As 7:3 lamina thickness was increased (Fig. 10), and increased burning rate resulted, the protrusion of the AP in the interface region became less and disappeared. The smooth bands also became localized very close to the interface planes. In that local region the AP surface was concave upward (evident in originals of Fig. 10), but the AP no longer protruded.

Burning Rate of Bimodal Propellants

The burning rates are shown in Fig. 11. The singular feature of the rate vs pressure of these propellants is a step in the burning rate-pressure curves. The

step occurs at higher pressure when the particle size of the fine fraction of AP is small. This trend is discussed further in a later section.

Discussion

The experimental results presented in this paper and its predecessor[10] represent parts of an evolving interplay between theory and experiment. Because of the complexity of the sandwich combustion process, it was judged at the outset that in the short term a realistic and comprehensive two-dimensional analytical model would be intractable. Accordingly the theory is based on qualitative arguments, and the experiments were designed to guide in formulation and evaluation of the theory. In this discussion, the qualitative theory will be presented in the form of a detailed description of a flame complex, accompanied by the basis for the details. To the extent that the basis for the details involves the present experimental results, the results will be discussed more fully after outlining the theory of the flame complex.

Before presenting the flame theory, attention is directed to five previously reported features of combustion of AP and AP composites that will be treated as axiomatic in the theory and subsequent discussion.

1. Ammonium perchlorate self deflagrates at pressures above about 2 MPa. This pressure limit is sensitive to temperature, AP purity and heat losses, presumably because of the rather modest flame temperature available to "drive" the combustion.[4,13,14,19,22,23-27]

2. Self deflagration of AP proceeds by a combination of a complex reaction in a surface liquid froth, along with a gas phase flame. Heat release occurs in varying degrees at both sites.[4,13,14,16,20,22,23,25] There are many references in the literature to condensed phase reactions, but such references do

not acknowledge the unequivocal evidence for the existence of the reactive froth or distinguish what is meant by condensed phase in that context. When the issue is reduced to one of real dimensions, the reaction region in the wave in the solid is so thin that it would be difficult to separate condensed phase, surface and gas phase reactions in the froth. However, the gas phase flame is generally treated as distinct from the froth under most conditions.[25]

3. Heat release in reactions between AP and hydrocarbon binders occurs primarily in the gas phase.[3-5,10-12,15-17,23,28] (Contrary views can be found in early literature, and are often argued by investigators whose primary investigative tools are thermal analysis instruments.)

4. Burning rates of the composite systems are dependent on the structural details of the systems. This is generally attributed to the effect of propellant microstructure on location of gas phase reaction sites (flames) (e.g., Ref. 1,8,15,29-33).

5. The gas phase oxidizer-binder flames consist of a leading edge portion involving vapors that have already mixed, and a trailing portion governed by continued diffusion of oxidizer and binder vapors. The leading edge portion is described as having the properties of a kinetically limited pre-mixed flame, and the trailing portion has the properties of a diffusion-limited flame.[1,9-12,15,21,23,31,32] Details and relative importance of the two portions of the flame are matters of speculation, but are examined later in the context of the present results.

Theory of the Flame Complex

Figure 12 is a sketch of the combustion zone of a burning sandwich, based on currently available evidence. The sketch represents only that portion of the combustion zone within about 150 μm of the plane of symmetry of the sandwich,

and represents conditions for thin-binder sandwiches burning at intermediate pressures (3 - 6 MPa). The numbers in circles in the sketch designate regions in the combustion zone with unique features, regions that will be discussed in detail in the following. It should be understood that the objective of discussing these features of the combustion zone is to obtain a reasonably complete description that can be used to understand detailed experimental observations (or design experiments to test the model), and to begin to explain such global combustion behavior as burning rate and dynamic response of combustion to oscillations in the flow environment.

Region (1) The Binder Lamina. The exposed binder lamina is recessed in quenched thin-binder sandwiches.[3,5,10-12,15-17,21,23,28] The appearance of the bottom of the recess suggests that it was molten during burning (most binders tested). The recessed condition could be an artifact of the quench, since real-time observations during burning do not have sufficient resolution to validate the quench test results. However, it seems clear that the thin binder laminae do not protrude during burning, as such a state would require that the protrusion be solid (in which case it would remain after the quench). Further, the speculation that the recess is caused by ejection of melt during quench[5] is put in doubt by the results with polysulfide binders, which burn without evidence of a melt but yield recessed binder laminae. Laminae of PBAN become somewhat protruding in the 50-90 μm range, and decidedly protruding with thicker laminae.

Region (2) The Interface Plane. The oxidizer-binder interface is never the leading edge of the burning front,[3,5,10,15,17,21,23,28] an observation that seems to rule out binder-oxidizer interfacial reactions as significant contributors to burning rate. The binder recess leaves a side wall that appears to be vertical in the interface plane, suggesting no AP decomposition in the recess. The bottom of the recess has the appearance of a miniscus, and there may be a film of binder on the sidewall of the recess (no evidence reported).

Region (3) Protruding AP-Smooth Band. Under all conditions tested (present work and Ref. 3,4,10,17,21,23,28,29), the AP deflagration in the region near the interface plane appears to be retarded relative to Region (4), and the AP surface there has a smooth quality suggestive of a different mode of decomposition than further out from the interface plane.[3-5,10-12,15,17,21,23,28] In earlier studies, these features were attributed to binder melt flow over the AP surface,[3,5,16,17,21,28] a conclusion that appears to be valid with thick laminae of meltable binder. However, the smooth band and protruding AP occur also with thin binder laminae where flow is less probable, with non-melting binders, and with a gold "heat sink" lamina in place of binder. As a result, it is theorized[21] that there is appreciable lateral heat flow into the endothermic binder, resulting in a lower AP surface temperature and a less exothermic or an endothermic surface decomposition (probably dissociative sublimation). This interpretation of Region 3 behavior has been supported recently by detailed calculation of heat flow in a two-dimensional model of the combustion of contacting slabs of oxidizer and fuel,[34] which shows that lateral heat flow into the binder lamina occurs.

Region (4) The Leading Edge in the AP. This region is generally located 25 -50 μm from the interface planes (present work and Ref. 3,5,10-12,15-17,21,28); a transition from smooth to "flakey" surface occurs here on quenched samples, indicating a transition in the nature of the surface decomposition to an exothermally reacting froth more typical of AP self-deflagration. Region (4) represents that point on the surface profile where the energy flux from gas phase flames, surface reaction, and two-dimensional heat flow in the solid (including binder) yield the highest heat flux in the direction of burning. At low pressure (e.g. < 1.4 MPa), the thickness of the thermal waves in the gas and solid are so

large that surface heat fluxes are more uniform, and localized effects such as the region (4) leading edge are inconspicuous. The transition in AP surface decomposition disappears as the pressure is reduced below the AP self-deflagration limit--the evidence of reacting froth no longer is present anywhere.[10,21,28,36,37]

Region (5) AP-Self-Deflagration. This region shows a surface essentially the same as for AP self-deflagration (including evidence of reactive froth), and surface regression rates are approximately the same as for self-deflagration.[15,21,22] At low pressure, the surface curves up toward vertical (Fig. 2a, d), reflecting the absence of sufficient heat flow from the AP-binder flame to sustain pyrolysis of the AP (the sandwiches were fuel-lean in overall stoichiometry). At high pressure (e.g., 8 - 14 MPa), the AP self-deflagration rate exceeds the sandwich rate (Fig. 5b) (which is now overwhelmed by the heat drain to the endothermic binder), and region (5) becomes the leading edge of the AP burning front (Fig. 2 c,f).

Region (6) The AP Flame. This flame is generally presumed to be present under self-deflagration conditions, and is postulated in propellant combustion models.[25] The chemistry and location of the flame are matters of speculation, as it appears to be too close to the surface to be resolved experimentally. The heat release of the AP self-deflagration apparently is apportioned between the surface froth and this flame, probably in a way that is sensitive to pressure and other factors affecting energy balance and surface temperature.[4,5,14,23,25] At this point it is not certain that the flame is a "sheet." The irregular and frothy nature of the AP surface probably gives rise to nonuniform flow and a correspondingly nonuniform flame. Combustion photography has been reported[4,37] to show turbulent flow from self-deflagrating AP, but it is doubtful

that the AP flame region is resolved in such photography, and the "turbulence" may be surface-coupled nonuniform flow. It has been suggested[4,14,25] that the heat release shifts to the gas flame (6) from the froth site (5) as pressure is decreased toward the self-deflagration limit, and that the limit is related to loss of the reacting froth.

Region (7) Leading Edge AP Flame. This is a continuation of the AP flame into a region that must receive some heat from the AP-binder flame, leading to the higher regression rate of the surface at (4). This, in turn, implies a higher surface temperature in region (4).

Region (8) Smooth Band Flame. This region is unique in that the vapors from the underlying surface (region (3)) are postulated to be different from those for the rest of the AP flame. Lacking any direct experimental evidence, speculation about the nature of the flame is a precarious exercise. Indeed, this region may not have an AP flame at all--an interpretation that would be consistent with the idea that loss of the surface froth reaction is associated with deflagration limits.[4,14,25] Diffusion of heavy fuel molecules into this region may actually suppress the AP flame; thus it may instead be a thermal and chemical induction zone for a later AP-binder flame in region (11).[10,11]

Region (9) Oxidizer-Fuel Diffusion Region. The dotted line in Fig. 12 represents the stoichiometric surface in a region of molecular diffusion of vapors. This "surface" bends out over the region above the oxidizer surface because the oxidizer is relatively dilute compared to the fuel. While the vapors are fairly hot (roughly 600° C as they leave the burning surface), the initial vapor mixing occurs in a region of high heat loss, so oxidizer-binder reactions cannot raise the temperature precipitously, and rates remain low until further out in the mixing region. This region (9) merges with region (8), and the uncertainty about an AP flame in region (8) translates into an uncertainty about details of region

(9). This same uncertainty has confronted propellant combustion modelers, who generally resolve it by somewhat arbitrary assumptions about flame structure. For the present, it will be assumed here that the AP flame reaches a quench limit somewhere in region (8), and that region (9) is a diffusion "fan" in which reaction rates are low because unfavorable balance of heat flow and insufficient mixing and chemical preparation of reactants prevent rapid temperature rise. However, one must keep in mind the qualitative features of regions (8), (9) and (10). Their interaction may be very pressure-dependent, and may oscillate during oscillations of the combustion environment.

Region (10 - 11) Kinetically Limited Leading Edge Flame. The diffusion region (9) prepares a flow in which an expanding oxidizer-fuel mixture develops by diffusion as convection carries the gases away from the surface. At some point in this mixing fan, the temperature becomes sufficient, relative to the two-dimensional heat flow, to support a flame. This flame is the leading edge of the diffusion flame, but unlike the diffusion flame (region 12), its position in the mixing fan is strongly dependent on reaction kinetics, standing as it does in a partially premixed flow. Accordingly, the name "kinetically limited leading edge flame," KLLEF, is used here to designate the flame. The existence and nature of such a flame in sandwich burning is simply postulated on fundamental grounds, since no direct observation has been made, due to the problem of spatial resolution. However, it is important to note that every free (unattached) diffusion flame has a kinetically limited leading edge of some kind. The KLLEFs are of particular importance in the present problem because, under some conditions, the majority of the oxidizer-fuel reaction occurs in the KLLEFs (no fuel left for the diffusion flames). Such (KLLE) flames have been observed in studies of flame propagation in stratified air-fuel mixtures at one atmosphere;[38,39] such flames show a leading edge at the stoichiometric surface

and trail off on the fuel-rich side (region (10) and oxidizer-rich side (region (11)). An analogous kinetically limited region of the flame is generally invoked also by modelers of propellant combustion,[1,29,30-33] and has been postulated in reports on combustion down the interface between oxidizer and fuel slabs.[9,10,11,22,23,31] Of particular note is the work of Fenn,[31] who discussed the nature and role of a kinetically limited reaction region he called the "phalanx flame." Because of its importance in the present work, the nature of the KLLEFs will be discussed in more detail later.

Region (12) Diffusion Flame. In the region downstream from the KLLEF (Fig. 12), continued reaction occurs as further interdiffusion of fuel and oxidizer vapors occurs. The temperatures are high due to heat release further upstream and diffusion of hot reaction products, and the reaction rate is consequently controlled by the rate of mixing, rather than reaction kinetics. The extent of this diffusion-limited portion of the flame is determined by the extent to which reactants have already been consumed by the KLLEF, and the extent of the fuel and oxidizer supply (i.e., thickness of the laminae that supply the reactants). According to classical theory, the diffusion flames locate themselves in such a way that oxidizer and fuel species will diffuse into the flames in stoichiometric proportions, with the reactants being fully converted to products at the flame surfaces. Thus the diffusion flame surfaces are continuations of the stoichiometric surfaces of regions (9); however there are no oxidizer species in the space between the flame surfaces in region (12), and no fuel species outside the flame surfaces. While this idealized "flame surface" approximation may not be quantitatively valid in the microflame situation of the present work, it is still a helpful concept for qualitative description of the situation.

Region (13) The Stoichiometric Tip. In Fig. 12 the flame complex is drawn for a thin binder lamina, with oxidizer laminae thick enough to represent a sample with oxidizer-rich overall stoichiometry. As a result, the diffusion flame sheets close over the fuel, yielding a flame tip that is referred to here as a stoichiometric tip. The region above the tip presumably contains little or no fuel species when the diffusion flame is present in region (12). However, later discussion will involve the implications of a situation where the KLLEFs and diffusion flames fail to be established in the mixing region, and the entire region (levels 9 - 12) is simply a two-interface diffusion region. In that situation, there are still stoichiometric surfaces and a stoichiometric tip, but the concentrations of fuel and oxidizer will not go to near zero at the stoichiometric surfaces as they do where the flames are present. In the configuration used here (thin-binder lamina), the mixture in the absence of a flame then will be increasingly oxidizer-rich as a function of distance above the stoichiometric tip, a condition that would be expected to affect the stability and location of any flame that might occur above the tip.

There are many features of sandwich burning that are not encompassed in the above description, features such as irregular burning at high pressure;[10] unsymmetrical burning with some binders;[5] melt flows with some binders and thick laminae;[3,5,16,17] possibility of turbulent smearing of the flame complex;[5] intermittency of flames;[5,10,15] and general breakdown of the two-dimensional symmetry of the flame. These features are probably each significant under some conditions, but were apparently not qualitatively important with the thin-binder PBAN sandwiches and test conditions used most extensively here. In this context, it is appropriate to note that many observations of these nonideal features of sandwich burning that have been reported in the past have been based on observational methods that are misleading (e.g., limited spatial resolution) or

test conditions and test samples not relevant to the studies reported here (e.g., thick binder). However, the issues raised merit continuing consideration in the future.

Interpretation of Results of Binder Substitutions

The foregoing qualitative theory was evolved as a framework in which to understand the emerging results of the present studies. One of the more conspicuous experimental results was the smooth surface quality and protrusion of the AP in Region 3. It was proposed that this region of the sample was deprived of heat by lateral transfer to the binder lamina, thus tending to hold down the surface temperature. Substitution of a nonconductive mica lamina led to elimination of the features of the profile attributed to the lateral heat drain, while substitution of a conductive gold lamina preserved these features. This result tends to support the lateral heat drain argument. At the same time, computer modeling of the heat flow problem was undertaken,[34] and results of numerical studies indicate that heat flow would indeed occur from oxidizer to binder under the conditions of AP-HC binder sandwich burning. As will be seen later, the results of sandwich burning rate measurements also indicate that lateral heat flow to the binder occurs. Given the rather marginal heat balance situation in AP self deflagration, it is then not surprising that the AP surface regression is retarded in Region 3. The persistent association of this with modified (smooth) surface quality suggests that the entire deflagration process is disturbed by the heat drain. This is interpreted here as a transition from normal self deflagration with an exothermic froth layer to simple dissociative sublimation. The resulting loss of surface heat release of course enhances the retardation of surface regression. In effect, the AP in Region 3 is behaving as if

it were below its self-deflagration limit, being pyrolized by heat flux from the gas phase flames.

In this context, it may be important to note again that the features of Region 3 have been attributed in the past to flow of molten binder over the AP surface. In experiments with binder laminae of thickness greater than 125 μm this interpretation is probably correct, at least with binders that yield high temperature surface melts. This is an unfortunate complication of the two dimensionality of the experiment, which must also affect the gas phase flame structure. This complication has been largely avoided in the presently reported work with thin PBAN binder laminae.

Interpretation of Deflagration Limit Results

The initial motivation for deflagration limit tests was to exploit an experiment that would be sensitive to the details of the flame complex and reaction kinetics. The systematic trends in the results (Fig. 6) at pressures below the AP self-deflagration limit posed a challenge that has yet to be exploited fully. However, some significant interpretation can be made now, interpretation that has been carried over to design of the bimodal propellant experiment and borne out by results of that experiment.

In interpreting the deflagration limit, one turns to arguments regarding the two-dimensional energy field, and what happens as the binder lamina becomes increasingly thin while approaching the quench point. Figure 13 shows the trend one would expect of the combustion zone details with binder thickness. As the binder thickness decreases, the mixing regions above the AP-binder interfaces move closer together and the stoichiometric tip retracts toward the surface. The total fuel supply decreases, with a corresponding decrease in available

combustion energy. Since this energy is dissipated two-dimensionally, one would expect burning rate and flame temperatures to drop off eventually with decreasing binder thickness. In such a situation, the energy balance ultimately becomes unstable and the "fire goes out." In the present situation, this may occur in either of two rather different ways that can be seen in Fig. 13. In part a, behavior at relatively low pressure is sketched. As binder thickness is reduced at constant pressure, the stoichiometric tip (Region 13 in Fig. 12) retracts until it is coincident with the oxidizer-binder KLLEFs. Any further decrease in binder thickness would place the KLLEFs in a location beyond the stoichiometric tip. The flames would not be stable in that location, because it is a region where fuel concentration becomes more fuel-lean with distance from the surface, with a corresponding decrease in available flame temperature. Thus, if the flame does not quench spontaneously by the time the stoichiometric tip retracts to the flame position, it will do so then. Quench due to tip retraction is more likely at low pressure, where the flame stands relatively far from the surface, and it is postulated that the steep, low-pressure part of the curves in Fig. 6 corresponds to quenches involving approach to the tip retraction. The dotted extension of the steep part of the curve at higher pressure is intended to show the locus of stoichiometric tip retraction that would result if the flame position were to continue to change with pressure in the manner of the low pressure curve.

At around 0.4 MPa the flame stability appears to become marginal before stoichiometric tip retraction. At higher pressures, the KLLEFs are located near the surface under stable burning conditions. By the time the binder thickness has decreased to 40 μm or so (Fig. 13b), the mixing regions and KLLEFs have substantially merged and the entire flame complex has become very small, but the KLLEFs still stand well down in the mixing regions. The limit of

flammability becomes dependent on the energy balance of this small flame burning down a narrow slot in the sample. With decreasing binder thickness, the burning rate drops off, and quench occurs when available heat from the flame can no longer support the losses. In the pressure range $0.4 < p < 2.0$, the approach to quench evidently does not depend on stoichiometric tip retraction, and the trend with pressure accordingly is different from that at lower pressure. The relative insensitivity to pressure suggests that approach to quench is governed by pressure insensitive diffusion processes, but this needs clarification by appropriate quantitative analysis. As in all quench events, the chemical kinetics become critical at the approach to the limit because of decreasing flame temperatures. In this limit domain, the final retreat of the flame may still be precipitated by withdrawal to the unstable region beyond the stoichiometric tip due to falling flame temperature, even in this higher pressure range. Presumably this is a "terminal aspect" of quench, which no longer dominates the pressure dependence of the quench limit. The effect of binder type on quench limit (Fig. 6) in this "diffusion dominated" domain appears to be related to the mode of decomposition of the polymer, and corresponding nature of the fuel molecules in the mixing region (9). PBAN binder is expected to yield relatively small vapor molecules, while HTPB will yield large molecules that must be further broken down to support a flame. It is postulated that this chemical induction process requires a longer time with HTPB than PBAN, with a correspondingly larger KLLEF stand-off distance and lower flame stability. The calculated stoichiometric flame temperature of the HTPB/AP flame is higher than that for PBAN/AP, a condition that adds plausibility to a fuel kinetics explanation of the difference in quench limit.

For the sake of completeness, it should be noted that above 2 MPa, sandwiches with thick oxidizer laminae burn regardless of binder thickness, because the AP burns as a monopropellant.

Sandwich Burning Rate

The experimental results indicate that the overall burning rate of the sandwich is dominated by the AP rate at pressures between 7 and 14 MPa, but that the AP-binder flame can have a significant effect at lower pressure (and, of course, dominate the rate below the AP self-deflagration limit). This is evident in Fig. 5, and is consistent with the larger features of quenched burning surfaces (Fig. 2). In terms of the flame complex in Fig. 12, one would expect that burning rate would be governed by heat release in a region of the flame complex relatively close to and on the burning surface. This region has been referred to[18,20,32,33] as the "propagation velocity controlling" (PVC) region. Under conditions where the sandwich rate is higher than the AP rate (Fig. 5b), the PVC region encompasses part of the binder-oxidizer flame, including the KLLEF. The PVC region is the region in which energy flow affects the temperature at the leading edge of the burning front. When the binder lamina is thick, the flame complexes above the two interface planes burn independently. There is a PVC region for each interface plane (dotted circles, Fig. 14a). In this situation, diffusion of heat (and chemical species in the gas) proceeds much as if the binder lamina were of infinite thickness, and the burning rate is independent of thickness. There is a threshold thickness of the binder lamina around 150 μm for PBAN binder ($1.4 < p < 5.5$ MPa) below which burning rate becomes sensitive to binder thickness (Fig. 5). This corresponds to the onset of interaction of the two PVC regions (Fig. 14b). Under these conditions, heat transfer from the AP laminae to the fuel lamina is decreased (because there is a smaller heat sink). The heat that is transferred is retained within the PVC region and is reflected as higher temperatures in the flame in the PVC region. In addition, fuel dilution of the mixing regions on the fuel-rich sides of the stoichiometric surfaces will be

reduced in the gas phase diffusion field. One would anticipate that the fuel-rich portion of the KLLEF (Region 10 in Fig. 12) would therefore be hotter and extend further into the fuel-rich region, with correspondingly larger heat release. In effect, the AP at the leading edge of the burning front experiences less lateral heat drain in the solid and more heat supply from the gas flame, with a corresponding enhancement of burning rate.

As binder thickness is reduced further, the total fuel supply is reduced until it is all consumed in the PVC region (i.e., none is left for the outer region of the trailing diffusion flame). Continued decrease in binder thickness thus eventually leads to decrease in heat release in the PVC regions, which are also substantially overlapping (Fig. 14c). Following the increase in burning rate caused by concentration of the two PVC regions, this trend to limitation in fuel supply must lead to a decreasing burning rate (Fig. 5). When pressures are above the AP self-deflagration limit, the sandwich rate will drop off with decreasing binder thickness until the AP deflagration rate is reached. At lower pressure, the rate will drop off until a combustion limit is reached (Fig. 6).

It is interesting to note that the foregoing arguments did not draw on the details of behavior in Regions 8 and 9 of Fig. 12, which have been described earlier as unknown. The results of quench tests indicate that the protrusion of AP near the interface planes and the characteristic smooth surface of the AP there persist over the whole range of test conditions and are evident even on spontaneous burnout tapered binder samples. This suggests that behavior in Regions 8 and 9 is not changing qualitatively. This, in turn, seems to be most compatible with the view that the AP vapors from this region are diluted by fuel vapors and fail to establish a near-surface AP flame, delaying heat release until the KLLEF location. At low pressure, the leading edge of the burning front (Region 4) receives heat primarily from the KLLEF and secondarily from the

trailing diffusion flame. Above the AP self-deflagration limit, the leading edge receives heat also from the AP reactions in Regions 4 - 7. Above about 7 MPa, the leading edge receives heat primarily from the AP reactions in Regions 4 - 7. Thus the character of the propagation velocity controlling region changes with binder thickness and pressure, and the burning rate trends suggest the nature of the changes (see later discussion of pressure dependence and Fig. 15 presented there).

Sandwiches With AP-Filled Binder Laminae

The range of test conditions in this investigation was rather limited, and the results consequently are probably more provocative than enlightening. The *investigation was done before the* burning rate study, and, in retrospect, the choice of 6.9 MPa for most of the tests probably limited the amount and interpretability of the results. However, they do merit some discussion.

The presence of a protruding region of the AP laminae on the tests with thin-binder lamina (Fig. 9, 10) indicates that lateral heat flow from the AP laminae to the filled binder lamina is still a factor in these tests. The smooth surface quality of the protruding region is still present. The peak of the protruding region is flattened off, compared to the pure-binder sandwiches. This suggests that the AP-binder flame is in closer proximity to that region, a conclusion that would be consistent with the fact that much of the oxidizer for that flame is pre-mixed in the binder lamina. The recess of the binder lamina and lesser recess of a thin region of the adjacent AP, in the test with 7:3 AP/binder mix in the binder lamina, seem to be indicative that the 7:3 mix burns on its own, a result consistent with past propellant experience (e.g., Ref. 40).

Increasing the thickness of the 7:3 AP-filled binder lamina resulted in an increase in sandwich burning rate, as revealed by the development of "V"-shaped surface profiles (Fig. 10). The burning rate of the 7:3 AP/binder mix alone was not determined, so it is not possible to determine from the present data whether the KLLEFs on the stoichiometric surfaces contributed significantly to the rate or not. The details of the flame structure over a 7:3 AP/binder propellant with 10 μm AP are also not known. However, the observations and interpretations of "smooth bands" near AP-binder interfaces suggest that the 10 μm AP particles sublime (i.e., the solid and surface processes in the "fuel" lamina are still endothermic). The results of the sandwich deflagration limit tests suggest that KLLEFs may not hold in the individual mixing fans of small AP particles, in which case the flame would be more nearly a flat pre-mixed flame over the 7:3 lamina. While these are rather speculative extensions of the results of tests on sandwiches with pure binder laminae, they are fundamental to the nature of the flame over the surface of the AP-filled binder laminae. The concept of stability of a KLLEF in the mixing fan from AP particles is pursued further in the bimodal propellant tests.

Interpretation of Results with Bimodal Propellants

The idea of stoichiometric tip retraction that was proposed to explain the pressure-sensitive parts of the deflagration limit curves (Fig. 6) has much broader relevance than the tapered sandwich experiment. In propellant combustion, there are stoichiometric surfaces and KLLEFs also, and the presence or absence of the KLLEFs on the stoichiometric surfaces would be expected to be important to the burning characteristics of the propellant. Of course, the issue is not a simple one of a deflagration limit, because the propellant surface is a chaotic array of oxidizer and binder surfaces of different dimensions. Yet one

may reasonably ask of each point on the surface, is there a KLLEF on the neighboring mixing region, or not? Presumably the answer will depend on pressure, and the dimensions of the local fuel and oxidizer surfaces. In that case, at low pressure, KLLEFs may be attached to individual mixing regions only at localities on the surface where relatively wide fuel and oxidizer surface elements are involved. As pressure is increased, conditions become more favorable for holding of KLLEFs, so these near-surface, high-temperature flamelets will be present on a larger range of oxidizer particle sizes. This has obvious implications for pressure dependence of burning rate, but involves a very different argument than those used in present burning rate models. In particular, it suggests a role of propellant microstructure that acts through pressure dependence of stability of near-surface microflames, rather than the usual mixing rate arguments.

In view of the difficulty of either observing the postulated microflame behavior or constructing analytical models to test the foregoing concepts, an experiment was sought in which the relevance of the concepts would be revealed by singular burning rate behavior. The burning rate tests on bimodal propellants were run for this purpose (Fig. 11). The virtue of bimodal propellants is that the burning surface can be viewed as consisting of "large" areas of oxidizer (each large particle) interspersed with areas of a binder-fine oxidizer mixture (this description applies if the particle size of the coarse oxidizer is much larger than the particle size of the fine oxidizer). In such a propellant, the question of KLLEF holding on the local mixing fans becomes less statistical, since mixing fans are divided into two categories (fine particle fans and coarse particle fans). The thesis of the experiment was that KLLEFs would hold on the coarse particle mixing fans over the whole range of pressures of interest, but hold on the mixing fans of individual fine oxidizer particles only at high pressure. If this reasoning were correct, one would expect that a curve of burning rate vs pressure would

show a break to higher burning rate at the pressure for establishment of KLLEF holding on fine particles. Further, one would expect the break in the curve to occur at higher pressure when the fine particles are smaller. The break in the curve would be sharp if the size distributions in the two oxidizer modes were very narrow, and less abrupt with broader size distributions.

The burning rate results in Fig. 11 constitute a test of the foregoing arguments, and show the breaks in the burning rate curves, with the predicted dependence on size of fine AP particles. These results not only support the mechanistic argument, but also provide an interesting means of tailoring burning rate. It should be recalled that the size distribution of the fine AP in these propellants was not particularly narrow; since the effect on burning rate is nonetheless clear cut, there appears to be considerable latitude for control of the burning rate curve by careful combinations of narrow-cut particle fractions.

The reader may have noted in the foregoing steady burning arguments that a deflagration limit concept previously called "stoichiometric tip retraction" was being used as a concept of KLLEF holding or nonholding. In the sandwich deflagration limit situation, the stoichiometric surfaces were closed over the binder in an oxidizer-rich system. In the propellant, the overall stoichiometry is fuel-rich, so one may imagine that the stoichiometric surfaces close over the oxidizer particles. The stoichiometric tips are close to the surface for small particles, far from the surface for large particles, a condition on which the rest of the argument is founded. However, the KLLEF holding-nonholding argument depends on the local oxidizer-fuel mixture being far enough from the stoichiometric condition to provide a strongly fuel-rich condition above the stoichiometric tips of the fine particles. If this condition were not met, the KLLEFs might hold at any height, i.e., the instability above the tips would be removed. This effect was demonstrated in the sandwich burning tests with AP-filled binder laminae, where a 1:1 AP:fuel ratio in the lamina appeared to yield no near surface flames in the 10 μm AP, while a 7:3 AP:fuel ratio caused the

thicker laminae to burn down ahead of the normal sandwich burning front in spite of the small AP particle size. It is not likely in this latter case that the KLLEFs were held on the individual mixing fans, but they nonetheless established locations close enough to the surface to dominate burning rate when the mixture was not too fuel-rich. In the case of the bimodal propellant tests, the mixture ratio of the binder-fine AP matrix was chosen to very fuel-rich.

Dependence of the Combustion Zone Details on Pressure

The model of combustion zone structure in Fig. 12 corresponds to the region of the sandwich and flame complex within 150 μm or less from the oxidizer-binder interface planes, and for a mid-range pressure (3-5 MPa). The differences in surface profiles with pressure have been described in the foregoing. These differences are indicative of substantial pressure dependence of the flame complex, and a proper use of the model of combustion zone structure would require consideration of these differences. Because pressure dependence is so important to combustion of propellants, the relevant material on pressure dependence of the sandwich flame complex is discussed more systematically here. The discussion is confined to thin-binder sandwiches and pure binders that do not produce melt flows onto the AP surface in such sandwiches. The discussion will address the regions 1-13 of Fig. 12 progressively. The pressure range covered is roughly 0.4 to 10 MPa.

Region 1. The binder lamina here is recessed relative to the immediately adjoining AP for lamina thickness less than 40 μm, and protrudes for binder thickness greater than about 80 μm. The trend has not been catalogued in detail, but is not notably pressure-dependent.

Region 2. The interface planes of this region do not show evidence of interfacial burning or other singular behavior over the range of conditions noted here.

Regions 3 and 4. The AP immediately adjoining the interface planes (Region 3) protrudes under all conditions (relative to the AP further from the interface). This is also the "smooth band" region. At low pressure, the protrusion is only marginally evident (0.1 MPa). At high pressure (see Fig. 3), the protrusion is dramatic (10 MPa).[10,11,15] The width and nature of the smooth band (and location of associated outer edge at Region 4) are relatively insensitive to pressure except to the extent that height of the region of AP protrusion changes. The lateral distance to the outer edge of the smooth band has not been determined systematically, but is typically in the 20-50 μm range. Thus the leading edge of the AP surface (Region 4) is always some distance from the interface plane, being located just beyond the smooth band. This is the point of maximum heat flux to the surface. At pressures above 7 MPa, the leading edge extends as a flat profile (Fig. 2) all the way to the outer edge of the sample, indicating that the AP burning rate exceeds the rate attributable to the sandwich (consistent with Fig. 5b).

Region 5. The pressure dependence of this region was described earlier. It behaves like self-deflagrating AP (above 2 MPa), and controls the burning rate above 7 MPa (Fig. 5b). Below 2 MPa the AP is pyrolized by the AP-binder flame.

From the results just summarized (1-5), it can be inferred that the maximum heat flux to the solid phase (and maximum AP surface temperature) occurs at Region 4. The temperature field in the solid must then be qualitatively similar to the sketch in Fig. 15. Such profiles are consistent with earlier observations of the boundary of the crystal phase change layer (240°C isotherm) in quenched samples,[3] and with profiles calculated in a two-dimensional model of

the two-slab burning problem.[34] These results seem to establish unambiguously that heat flows from the AP to the binder over the whole pressure range.

The extent of the region in the AP in which lateral heat transfer is important must be of the same order as the thermal wave thickness in the solid. The thickness of this heated layer can be calculated from estimated thermal properties of the ingredients, surface temperatures and burning rates (which are pressure-dependent). The thickness can also be estimated from experimental observations of the thickness of the crystal phase change layer on quenched AP samples.[3,39] The latter results show that the temperature falls from 550-600°C down to 240°C in a distance of 8 μm at 10 MPa, and a distance of 58 μm at 1 MPa. These results are consistent with estimates based on thermal properties and burning rates. The resulting dimensions are of the same order as the width of the region of retarded AP regression and smooth band (Region 3), indicating not only that lateral heat transfer to the binder is present (based on isotherm profiles), but is effective in the dimensional domain postulated in the model. The total effect of the lateral heat drain from the AP on the surface regions depends upon its effect on the flame complex (heat source distribution). Thus the total effect of pressure on the condensed phase temperature field or surface profile cannot be estimated without consideration of the pressure dependence of the flame complex. Judging from the wide change in surface profile in Region 3 (Fig. 3 and Ref. 15) over the pressure range (especially above 7 MPa), the pressure dependence of the heat source distribution is a major factor in determining this part of the surface profile and temperature field in the solid.

Region 6. The pressure dependence in this region is simply that of the AP self-deflagration flame.[25] It seems likely that more of the total exothermic reaction of the AP occurs in this flame at low pressure than at high pressure, since evidence of the froth reaction on quenched samples becomes minimal as

the low pressure self-deflagration limit of the AP is approached. Below that pressure, the gas phase AP flame may still be present in locations where heat losses are low and heat flow from the oxidizer-binder flame can support the AP flame. Since no direct observations of the AP flame have been reported, the above arguments are inferences from indirect evidence, and are, at best, of only qualitative validity.

Region 7. The qualitative argument concerning the AP flame in Region 6 is also relevant to Region 7, but in this region there is no doubt that the flame receives heat from the AP-binder flame, because the burning rate of the underlying AP is higher than the AP self-deflagration rate (Fig. 5b) at pressures below about 7 MPa. Above this pressure the AP combustion is not enhanced locally by the oxidizer-binder flame, and Regions 4 and 7 cease to have unique existence (the curves in Fig. 5b converge into a single curve, which is the AP self-deflagration rate). The minimum pressure for the AP flame to be present at Region 7 is not known; below the AP self-deflagration limit, its presence would depend on the presence and condition of the AP-binder flame.

Region 8. As noted earlier, the status of the AP flame in this region is uncertain at all pressures. From the extreme protrusion of the AP in this region at high pressure, it seems likely that there is no local AP flame, i.e., the AP flame in Region 7 encounters a quench limit on the Region 8 side due to lateral heat drain into the solid and reduced heat supply from the AP-binder flame. It is this reasoning that led to the speculation earlier that there was no AP flame in Region 9. The evidence for this is convincing at high pressure because of the extreme AP protrusion, but presence of a quench limit for the AP flame between Regions 7 and 9 seems plausible also at lower pressures. This hypothesis is supported by the relatively low pressure sensitivity of the related features in the underlying surface (smooth band and AP protrusion) in the lower pressure range.

Region 9. This region is a mixing "fan" between oxidizer and fuel flow. Such regions occur in pairs, which interact increasingly with each other at greater distance out from the surface. While these interactions have been stressed in explaining burning rate trends and deflagration limits, a quantitative analysis of such pairs of mixing fans is not available. Some insight into pressure dependence of the flame complex can be gained by examining a simpler, more tractable representation of the single mixing fan problem. For that purpose, it will be assumed that oxidizer and binder vapors leave the surface as parallel flows of equal velocity, v, and temperature, and that this condition is preserved out to the KLLEF (Regions 10,11). In that case, a layer of gas emerging from the solid at a specific time can be located later at a definite "y" position (Fig. 16) that is proportional to time. It will be assumed that mixing of the two gases in a convected layer proceeds by molecular diffusion, and only in the lateral direction. Using the equations for a binary system with diffusion coefficients $D_{12} = D_{21}$, diffusion in the x direction in a convective layer proceeds according to Fick's Law

$$YV = - D \frac{dY}{dx} \tag{1}$$

where Y is a mass fraction of one of the gases and V is diffusion velocity. For a given volume (length) element in the moving layer of gas, conservation of a specie Y requires that

$$\frac{dY}{dt} = - D \frac{d^2Y}{dx^2} = - \frac{d^2Y}{d\xi^2} \tag{2}$$

where

$$\xi \equiv xD^{-1/2} \tag{3}$$

For this purpose, note that the initial condition on Y is the same for all pressures, i.e., $Y_o = 1$ at the oxidizer surface and $Y_f = 1$ at the fuel surface. The initial mixing is primarily close to the interface plane where concentration gradients are high, and the boundary conditions at "large" x have little effect. Assuming this to be valid in all of Region 9, the solutions to Eq. (2) in the region of interest are closely approximated by a single pair of time-dependent mass fraction profiles (one for Y_o and one for Y_f),

$$Y = Y(\xi, t) = Y(\xi, \frac{y}{v}) \tag{4}$$

where y/v reflects the convection of the layer outward from the surface at velocity v.

To the extent that pressure does not affect the validity of assumptions about boundary conditions at "large" x, a set of solutions, $Y = Y(\xi)$, corresponding to various values of t, applies for all pressures; the pressure dependence is contained in the relation of ξ to x, and of t to y which are necessary to convert Eq. (4) into concentration fields in x and y coordinates. The relation of ξ to x Eq. ((3) depends on pressure through D, which is inversely proportional to p.[41] Thus

$$x = (K_1 p^{-1/2})\xi \tag{5}$$

The y position for a given t is given by

$$y = vt \tag{6}$$

where v is the velocity from the surface, and is pressure dependent. Applying mass continuity at the surface, and assuming the burning rate depends on pressure according to

$$r = Cp^n \tag{7}$$

(*where n is typically between 0.2 and 0.5*), continuity requires

$$v \rho_g = r \rho_s$$

$$v = K_2 p^{n-1}$$

and

$$y = K_2 p^{n-1} t \tag{8}$$

Suppose one considers mixing fans at different pressures, and seeks the concentration profile in each fan that corresponds to a specific convection time t_1. Equation (8) indicates the y coordinate of that concentration profile, Eq. (4) gives the concentration profile for that time t_1 (in ξ coordinate), and Eq. (5) provides the conversion of the profile to the x coordinate. *Examining these* equations, the t_1 profile moves in closer to the surface as pressure increases, and the profile contracts in the x direction. This pressure dependence of the mixing region is illustrated qualitatively by the sketch in Fig. 17. The span of the layers sketched in Fig. 17 corresponds to a specific span of ξ for the time $t = t_1$, and corresponding mass fraction profile $Y_{t_1}(\xi)$. However, the mass flow through the

segments at different pressures are not the same. Thus, if the width of the segment is designated by "w",

$$\overset{c}{m} = \rho v w$$

which depends on pressure according to

$$\overset{c}{m} \alpha p \cdot p^{n-1} \cdot p^{-\frac{1}{2}} = p^{n-\frac{1}{2}} \tag{9}$$

The reason for addressing the trend of conditions in a specific span of $Y_{t_1}(\xi)$ as a function of pressure is explained in the following.

Region 10 - 11. This is the kinetically limited flame in the mixing region. Its position and span are important to the whole combustion region. Its position is pressure dependent to the extent that pressure affects reaction rates, but the net effect depends also on the fact that an advance of the flame into the mixing region (lower value of t and y/v in Eq. (4)) means advance into a region of steeper mixing profiles and less extensively mixed gases. In this situation of two-dimensional heat losses, further advance into the mixing fan is thus limited by a decreasing reactive mixture in the presence of relatively unchanged heat losses, i.e., the mixing field in Region 9 limits the extent of the kinetically controlled response to pressure change.

Region 10 - 11 refers to a transverse flame in the mixing region. While there is no direct observational data about such micro flames, their behavior will be argued here on the basis of more traditional theory and observation of macro flames. The "KLLEF" is probably crescent-shaped[38,39] with leading edge on the stoichiometric surface. It extends outward laterally into the mixing region to an

extent limited by flammability limits in the off-stoichiometric mixture. Presumably, the location (y-coordinate) and span (width in the mixing field) are dependent on pressure. The flame is kinetically limited in the sense that it stands in a pre-mixed flow, but that flow is a diffusion fan, and the response of the flame to pressure (e.g., standoff distance from the surface) depends also on the state of mixing as a function of y. This will be examined by a very simplified model in the following.

Suppose that, under a given set of conditions, the KLLEF is approximated by a planar flame analogous to the mixing layers described for Region 9 (Fig. 17). Then a KLLEF would be associated with a specific concentration profile (Eq. (4)), flow time from the surface, and span of ξ corresponding to fuel-rich and oxidizer-rich flammability limits. At a higher pressure, assume that these same concentration conditions determine the flame location and span (i.e., that the position of the flame is dominated by adiabatic flame temperature). Thus the preceding description of pressure dependence of segments of the mixing layer applies also to the KLLEF, and the flame position and span are given by applying Eqs. (5) and (8) to the t and ξ span of the flame at the higher reference pressure. Thus the flame would move closer to the surface and contract laterally as pressure increased in the manner described for the mixing fan analysis and Fig. 17.

Described in the foregoing terms, one might ask, in what way does the description reflect the "kinetically limited" aspect of the flame? This is embedded in the assumption that the flame is postulated to move in such a way as to maintain the same flame temperature profile and chemical induction time at all pressures (neglecting heat losses). This seems like a reasonable approximation in view of the exponential temperature dependence of reaction rate. However, the collision rate does increase with pressure, and the flame probably advances more than the amount predicted by Eq. (8). In doing so, the

span of the flame would also be reduced, and the mass flux through the flame would be reduced more than indicated by Eq. (9). Thus the advance of the flame with increasing pressure also contracts the flame and decreases the total heat release. Given the two-dimensional nature of the heat transfer from the flame, a more complete two-dimensional analysis would be required to quantify the argument further. In such an analysis it would be necessary to consider more carefully the boundary conditions. We have argued earlier that interaction of adjoining mixing fans is an important factor in the effect of binder thickness on burning rate and deflagration limits, indicating the necessity to quantify the above simplistic argument for realistic description of pressure dependence of KLLEFs with thin-binder sandwiches and/or low pressures.

Interaction of Regions. The examination of pressure dependence of the combustion by looking at one Region at a time was helpful from the standpoint of ordering the information on these individual aspects of the flame complex, but the combustion is a pressure-dependent interplay of the processes in each region. This interplay has been drawn upon to explain the results of the various experiments reported here (indeed, the experimental results contributed to clarification of interactions and their pressure dependence). However, it may be helpful to bring this information together in a systematic description of pressure dependence of the overall combustion zone. In doing this, it is helpful to refer back to discussion of the results in Fig. 5 for orientation. It was argued there that adjoining mixing fans do not interact when the binder thickness is > 150 μm, thus permitting consideration of the pressure dependence of the mixing region (Region 9) and KLLEF region (Region 10-11) in the manner presented above. However, the trend to increasing burning rate with decreases in binder thickness in the range $150 \rightarrow 65$ μm is attributed to increasing proximity (interaction) of

the flame complexes of the two interface planes (Fig. 14). This burning rate response to binder thickness is clearly pressure-dependent (Fig. 5), and it is reasonable to assume that this is due to changes in the interaction of the adjoining interface flame complexes. These interaction effects can be more decisively explained now that the pressure dependence of the individual regions has been clarified.

For large binder thickness, the change in combustion zone microstructure with pressure is indicated qualitatively by Fig. 18a, and presumably conforms to the trend discussed above. At high pressure, the AP simply runs away from the interface-AP-binder flame complexes, which are noninteractive at this binder thickness. At intermediate pressure, the combination of AP flame and AP binder flame determines the overall rate, but the heat drain to the binder slows the burning some. Below the AP self-deflagration limit, the two AP-binder flames dominate burning noninteractively; some heat release in a local AP flame may occur over the leading edge region.

With binder laminae in the 65-85 μm range, the experimental results indicate that the AP-binder flame contributes substantially to the burning rate at pressures below 7 MPa, so that Region 4 controls the burning rate. As a result, the surface profiles show a straight incline of the AP surface in Region 5, and the reactions there and in the flame (Region 6) conform to normal AP self-deflagration. The enhanced importance of Region 4 to burning rate at lower pressure with this binder thickness is interpreted as being a result of interaction of the mixing fans and elimination of heat loss to excess fuel flow between the PVC regions. The pressure dependence of the flame complex is shown in Fig. 18b. Above 7 MPa, heat drawn to the binder still retards the AP regression locally, and the AP-binder flame, while close to the interface plane, is too small and

stands too far from the rest of the AP surface to affect the rate (i.e., Region 4 ceases to exist and Region 5 controls the rate). At lower pressure, the AP flame moves out enough so that the heat from the AP-binder flame becomes a significant factor and Region 4 dominates the burning rate. The mixing region analysis suggests that under these conditions most of the binder vapors pass through the KLLEFs, and the diffusion flames (Region 12) are thus limited to the region immediately beyond the KLLEFs. To the extent that this is true, the stoichiometric tip (Region 13) is located fairly near to the KLLEFs, and probably in the PVC region. At low pressure, the burning becomes increasingly dependent on the AP-binder flames because of the drop-off in AP self-deflagration. The AP/binder flames stand far enough from the surface to approximate a planar heat source as "seen from" Regions 1-4. The thick thermal wave in the solid implies more nearly one-dimensional temperature profiles in the solid. However the difference in kinetics of binder and AP pyrolysis and thermal properties requires that lateral heat flow continue, and the smooth band and retarded AP (Region 3) are still evident (to a lesser degree) down to the lowest pressures tested. At the low pressure limit for burning (Fig. 6), the KLLEFs apparently have moved out to the stoichiometric tip; as noted earlier, the flame will not hold beyond this point (lower pressure) so that a pressure limit is established.

When the binder lamina is very thin (e.g., < 40 μm (Fig. 18c), the mixing fans are substantially merged as are the KLLEFs (Fig. 14). The earlier arguments regarding pressure dependence of the mixing fan and KLLEF position cannot be applied with confidence because the boundary conditions on the fuel side affect the mixing field in a different and more complex way. Specifically, the limited supply of fuel and proximity of the mixing fans to each other causes the stoichiometric surfaces to be localized closer to the plane of symmetry, and moves the stoichiometric tip closer to the surface. The smaller, more centrally

located flame contributes less to the burning rate, and the decreased height of the stoichiometric tip and "poor energy budget" causes the deflagration limit to occur at a higher pressure (Fig. 6).

Comment

The practical purpose of studies of sandwich burning is to clarify the controlling mechanisms of composite propellant burning. There should be no illusions about the strategy. It cannot clarify all relevant aspects of propellant combustion, and the difficulties of studying propellants do not all go away when one turns to sandwich studies. The present results do indicate that a good deal can be learned about combustion zone structure in the context of the "simple" sandwich system. It should be no surprise that the resulting view of the combustion zone is two-dimensional, not one-dimensional, since the sandwich system is two-dimensional. However, it should be recognized that those features of the sandwich combustion zone that are within 50 μm of the interface planes between laminae have their counterpart on propellant surfaces, where oxidizer crystals are typically 150 μm in diameter. If we are to understand composite propellant combustion, we must deal with the same multi-dimensional features of the combustion zone that are present in sandwich burning. The sandwich results show the gas phase, surface and subsurface processes to be all multi-dimensional, and all closely coupled. Pyrolysis of the binder is aided by lateral heat flow from the oxidizer. The heat drain from that region of the oxidizer causes a local change in the mode of vaporization of the oxidizer, and a change in site of its heat release. This anomalous vaporization must have some effect on the near surface oxidizer-binder flame. While there are conditions (e.g., high pressure)

where this locally coupled aspect of the behavior in the PVC region may not be important to the mean burning rate, it appears that under most rocket motor conditions, realistic modeling of either steady or unsteady combustion of AP-HC binder propellants must address the three-dimensionally coupled nature of the processes in the entire combustion wave. It doesn't require much imagination to see the same surface features on quenched propellant samples (Fig. 19) that have been discussed here for sandwich burning. By the same token, the structure of the flame complex can also be postulated with reasonable confidence (Fig. 20). In the case of the propellant, some further consideration must be given to propagation of the flame between particles,[42] and to the question of the least-time path of the burning front through the more complicated propellant matrix.[15]

References

1. Beckstead, M. W., Derr, R. L., and Price, C. F., "A Model of Solid Propellant Combustion Based on Multiple Flames," AIAA Journal, Vol. 8, Dec. 1970, pp. 2200-2206.

2. Powling, J., "Experiments Relating to the Combustion of Ammonium Perchlorate-Based Propellants," Proceedings of the 11th Symposium (International) on Combustion, 1966, The Combustion Institute, Pittsburgh, Pa., 1967, pp. 447-456.

3. Hightower, J. D. and Price, E. W., "Experimental Studies Relating to the Combustion Mechanism of Composite Propellants," Astronautica Acta, Vol. 14, 1968, pp. 11-21.

4. Hightower, J. D., Price, E. W., and Zurn, D. E., "Continuing Studies of the Combustion of Ammonium Perchlorate," CPIA Publication No. 162, Vol. 1, December 1967, pp. 527-534.

5. Boggs, T. L. and Zurn, D. E., "The Deflagration of Ammonium Perchlorate-Polymeric Binder Sandwich Models," Combustion Science and Technology, Vol. 4, 1972, pp. 279-292.

6. Brown, W. E., Kennedy, J. R., and Netzer, D. W., "An Experimental Study of Ammonium Perchlorate-Binder Sandwich Combustion in Standard and High Acceleration Environments," Combustion Science and Technology, Vol. 6, 1972, pp. 211-222.

7. Abraham, M., III and Netzer, D. W., "Nonmetallized Solid Propellant Combustion in Standard and High Acceleration Environments," Combustion Science and Technology, Vol. 11, 1975, pp. 75-83.

8. Nadaud, L., "Models Used at ONERA To Interpret Combustion Phenomena in Heterogeneous Solid Propellants," Combustion and Flames, Vol. 12, 1968, pp. 177-195.

9. Ermolaev, B. S., Korotkov, A. I., and Frolov, Yu. V., "Laws of Combustion of a Solid Propellant Sandwich," Fizika Goreniya i Vzryva, Vol. 6, July-Sept. 1970, pp. 277-285.

10. Price, E. W., Handley, J. C., Panyam, R. R., Sigman, R. K. and Ghosh, A., "Combustion of Ammonium Perchlorate-Polymer Sandwiches," AIAA Journal, Vol. 19, March 1981, pp. 380-386.

11. Price, E. W., Sigman, R. K., and Panyam, R. R., "Combustion Mechanisms of Solid Propellants," Georgia Institute of Technology, Atlanta, Ga., September 1981.

12. Price, E. W., Panyam, R. R., and Sigman, R. K., "Microstructure of the Combustion Zone: Thin-Binder AP-Polymer Sandwiches," CPIA Publication No. 329, Vol. 1, Nov. 1980, pp. 37-51.

13. Hightower, J. D. and Price, E. W., "Combustion of Ammonium Perchlorate," Proceedings of the 11th Symposium (International) on Combustion, 1966, The Combustion Institute, Pittsburgh, Pa., 1967, pp. 463-472.

14. Boggs, T. L., Price, E. W., and Zurn, D. E., "The Deflagration of Pure and Isomorphously Doped Ammonium Perchlorate," Proceedings of the 13th Symposium (International) on Combustion, 1970, The Combustion Institute, Pittsburgh, Pa., 1971, pp. 995-1008.

15. Price, E. W., Handley, J. C., Strahle, W. C., Sheshadri, T. S., Sigman, R. K., and Ghosh, A., "Combustion Mechanisms of Solid Propellants," Georgia Institute of Technology, Atlanta, Ga., Sept. 1980.

16. Boggs, T. L., Zurn, D. E., Strahle, W. C., Handley, J. C., and Milkie, T. T., "Mechanisms of Combustion," Naval Weapons Center, NWC TP 5514, 1973.

17. Varney, A. M. and Strahle, W. C., "Experimental Combustion Studies of Two-Dimensional Ammonium Perchlorate-Binder Sandwiches," Combustion Science and Technology, Vol. 4, 1972, pp. 197-208.

18. Price, E. W. and Sambamurthi, J. K., "Dependence of Burning Rate of AP-Polymer Sandwiches on Thickness of the Binder Laminae," CPIA Pub. No. 383, Vol. I, October 1983, p. 223

19. Boggs, T. L., Zurn, D. E., and Netzer, D. W., "Ammonium Perchlorate Combustion: Effects of Sample Preparation; Ingredient Type; and Pressure, Temperature and Acceleration Environments," Combustion Science and Technology, Vol. 7, 1973, pp. 177-183.

20. Price, E. W., Panyam, R. R., Sambamurthi, J. K., and Sigman, R. K., "Combustion of Ammonium Perchlorate-Polymer Sandwiches," Annual Report on Office of Naval Research Contract N00014-79-C-0764, Georgia Institute of Technology, Atlanta, Ga., February 1983.

21. Price, E. W., Panyam, R. R., Sambamurthi, J. K., and Sigman, R. K., "Combustion of Ammonium Perchlorate-Polymer Sandwiches," 19th JANNAF Combustion Meeting, CPIA Publication No. 366, Vol. I, October 1982, p. 81.

22. Boggs, T. L., "Deflagration Rate, Surface Structure, and Subsurface Profile of Self-Deflagrating Single Crystals of Ammonium Perchlorate," AIAA Journal, Vol. 8, No. 5, May 1970, p. 867.

23. Price, E. W. and Flandro, G. A., "Workshop Report: Combustion Zone Microstructure and Flow Effects," CPIA Publication No. 366, Vol. I, October 1982, p. 73.

24. Cohen Nir, E., "An Experimental Study of the Low Pressure Limit for Steady Deflagration of Ammonium Perchlorate," Combustion and Flame, Vol. 20, 1973, pp. 419-435.

25. Guirao, C. and Williams, F. A., "A Model for Ammonium Perchlorate Deflagration between 20 and 100 atm," AIAA Journal, Vol. 9, July 1971, pp. 1345-1356.

26. Boggs, T. L. and Zurn, D. E., "The Temperature Sensitivity of the Deflagration Rates of Pure and Doped Ammonium Perchlorate," Combustion Science and Technology, Vol. 4, 1972, pp. 227-232.

27. Levy, J. B. and Friedman, R., "Further Studies of Pure Ammonium Perchlorate Deflagration," Proceedings of the Eighth Symposium (International) on Combustion, The Combustion Institute, Williams and Wilkins Co., Baltimore, 1962, p. 663.

28. Hightower, J. D. and Price, E. W., "Two-Dimensional Experimental Studies of the Combustion Zone of Composite Propellants," CPIA Publication No. 105, Vol. 1, May 1966, pp. 421-435.

29. Cohen, N. S., "Review of Composite Propellant Burn Rate Modeling--A Review," 17th Aerospace Sciences Meeting, Jan. 15-17, 1979, New Orleans, La., AIAA Paper 79-0160.

30. Summerfield, M., Sutherland, G. S., Webb, M. J., Taback, H. V., and Hall, K. P., "Burning Mechanism of Ammonium Perchlorate Propellants," Solid Propellant Rocket Research, Progress in Astronautics and Rocketry Series, Vol. 1, Academic Press, New York, 1960, pp. 141-182.

31. Fenn, J. B., "A Phalanx Flame Model for the Combustion of Composite Solid Propellants," Combustion and Flame, Vol. 12, June 1968, pp. 201-216.

32. Belyaev, A. F. and Bakhman, N. N.,"Theory of Burning Powders and Solid Rocket Propellants (Review)," Combustion, Explosion and Shock Waves, Vol. 2, Winter 1966, pp. 1-17.

33. Bakhman, N. N., and Librovich, V. B., "Flame Propagation Along Solid Fuel-Solid Oxidizer Interface," Combustion and Flame, Vol. 15, No. 2, October 1970, pp. 143-155.

34. Panyam, R. R., "Combustion at the Interface of an Oxidizer-Fuel Slab System," Ph. D. Thesis, Georgia Institute of Technology, Atlanta, Ga., June 1983.

35. Handley, J. C., Price, E. W., and Ghosh, A., "Combustion of Non-Aluminized Binders in Tapered Sandwiches," 16th JANNAF Combustion Meeting, CPIA Publication No. 308, Vol. 2, October 1979, p. 127.

36. Boggs, T. L., Kraeutle, K, J., "Role of the Scanning Electron Microscope in the Study of Solid Rocket Propellant Combustion, I. Ammonium Perchlorate Decomposition and Deflagration," Combustion Science and Technology, Vol. 1, 1969, pp. 75-93.

37. Murphy, J. L. and Netzer, D. W., "Ammonium Perchlorate and Ammonium Perchlorate-Binder Sandwich Combustion," AIAA Journal, Vol. 12, No. 1, Jan. 1974, pp. 13-14.

38. Phillips, H., "Flame in a Buoyant Methane Layer," Proceedings of the Tenth Symposium (International) on Combustion, The Combustion Institute, Pittsburgh, Pa., 1965, pp. 1277-1283.

39. Ishakawa, N., "Flame Structure and Propagation Through an Interface of Layered Gases," Combustion Science and Technology, Vol. 31, 1983, pp. 109-117.

40. Schmidt, W. G., Lovine, R. L., and Poynter, A. L., "Zirconium/Aluminum Combustion," AFRPL TR-81-19, April 1981.

41. Williams, F. A., "Combustion Theory: the Fundamental Theory of Chemically Reacting Flow Systems," Addison-Wesley Publishing Company, Reading, Mass., 1965.

42. Strahle, W. C., "Some Statistical Considerations in the Burning of Composite Solid Propellants, AIAA Journal, Vol. 16, No. 8, Aug. 1978, pp. 843-847.

Table I

Test conditions for sandwich tests with AP-filled binder laminae
10μm AP, lamina thickness approximately 80μm, unless noted otherwise

Serial No.	Variable \ Pressure	1.4 MPa (200 psi)	4.2 MPa (600 psi)	6.9 MPa (1000 psi)
1	Control - PBAN binder	X	X	X
2	1/1 AP/PBAN	X	X	X
3	7/3 AP/PBAN	X	X	X
4	Control - PBAN Binder	X	X	X
5	1/1 AP/HTPB	X	X	X
6	7/3 AP/PBAN lamina 40μm thick			X
7	7/3 AP/PBAN lamina 140μm thick			X
8	7/3 AP/PBAN lamina 65μm thick			X

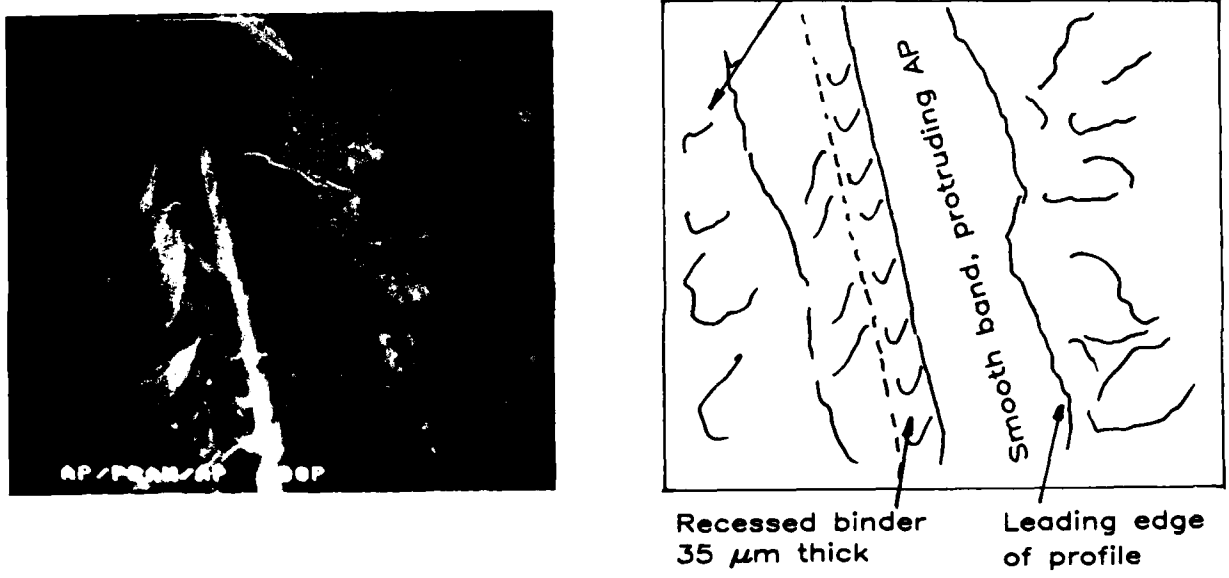

Fig. 1 Surface of a quenched "sandwich" of AP-PBAN-AP laminae (region of surface near binder lamina).

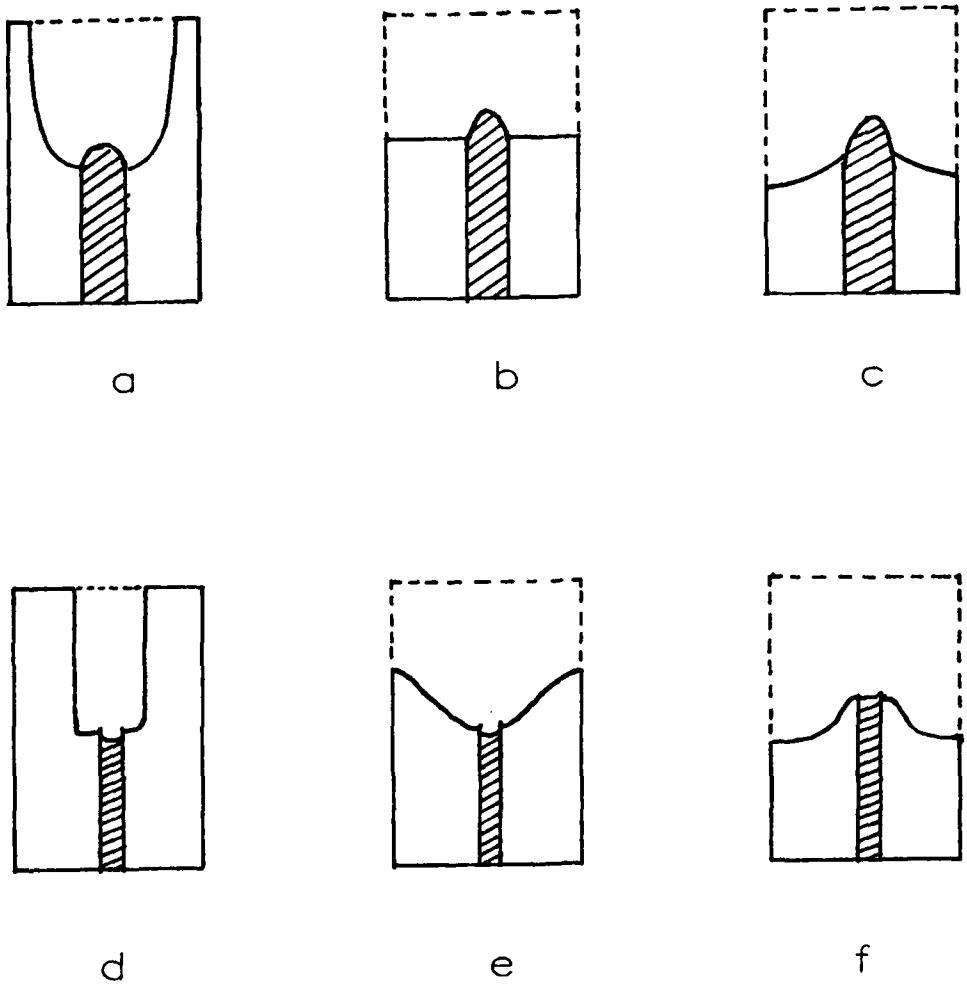

Fig. 2 The larger features of burning surface profiles.

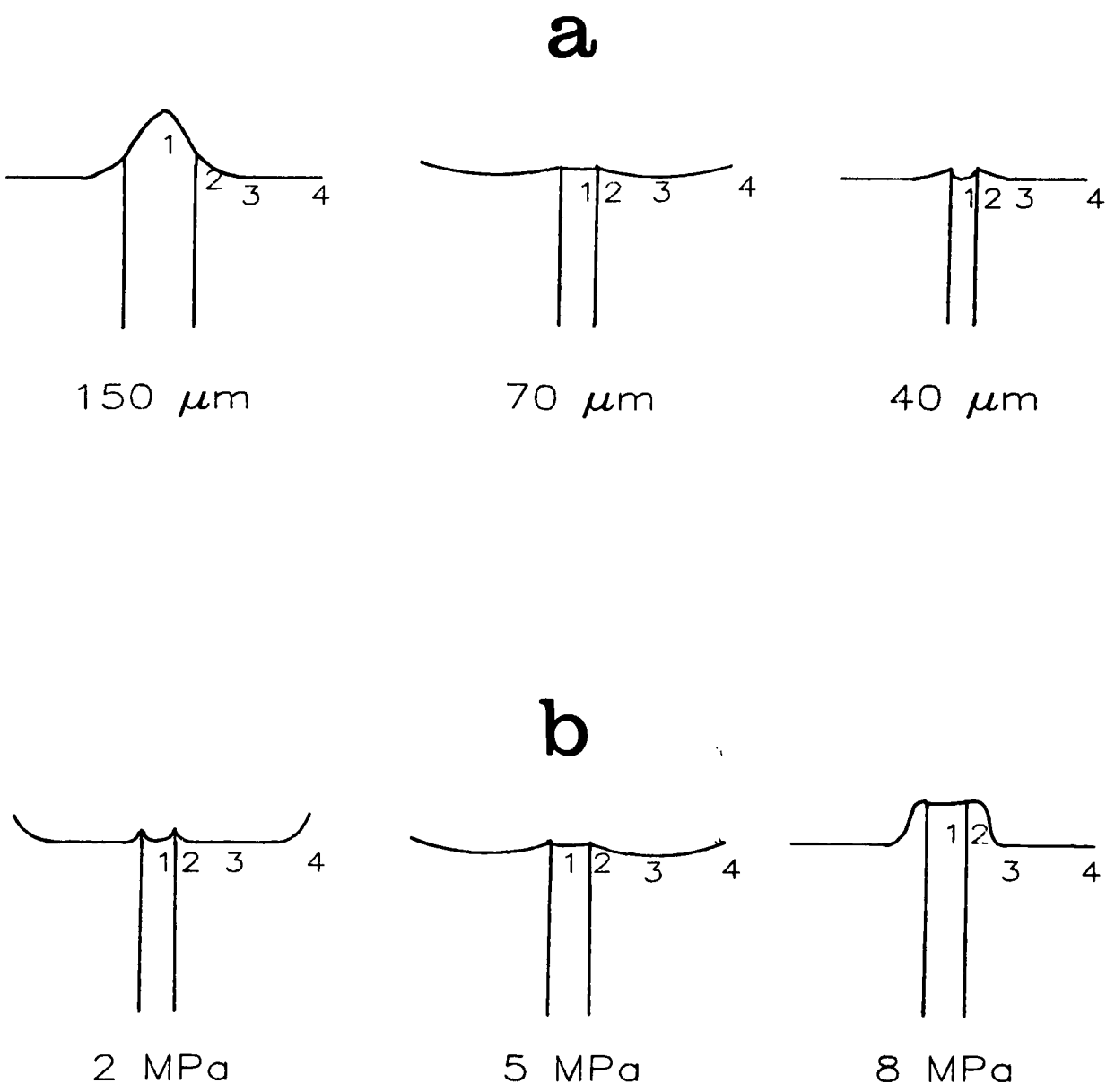

Fig. 3 Details of surface profiles in the region near the lamina interface planes. (PBAN binder).

a) Effect of binder thickness at 5 MPa.
b) Effect of pressure for binder thickness of 70 μm.

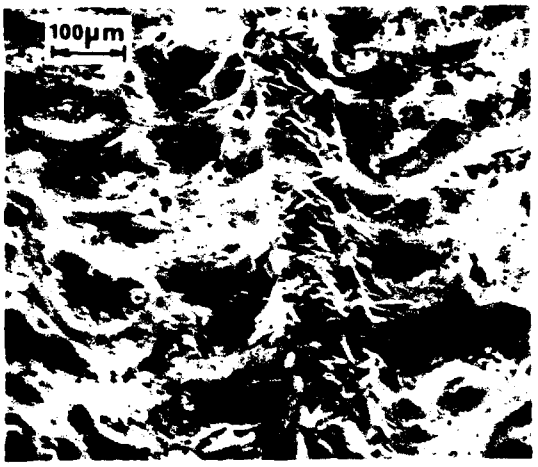

a

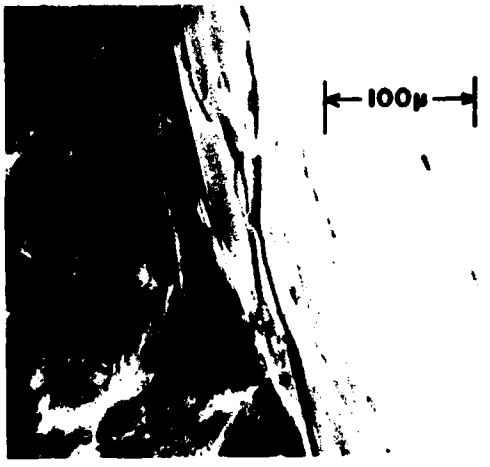

b

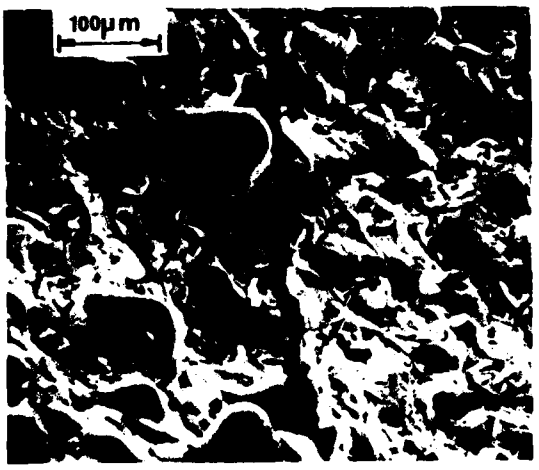

c

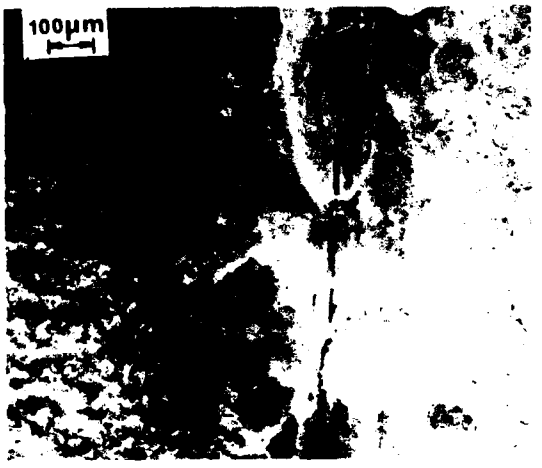

d

Fig. 4 Quenched surfaces with various substitutions for the binder lamina (4.2 MPa)
a) Control test (PBAN binder)
b) Mica lamina (area on the right is the protruding lamina, showing some flaking of the mica)
c) AP lamina in direct contact (separation occurred during post-test handling)
d) Gold lamina (15 µm; not visible)

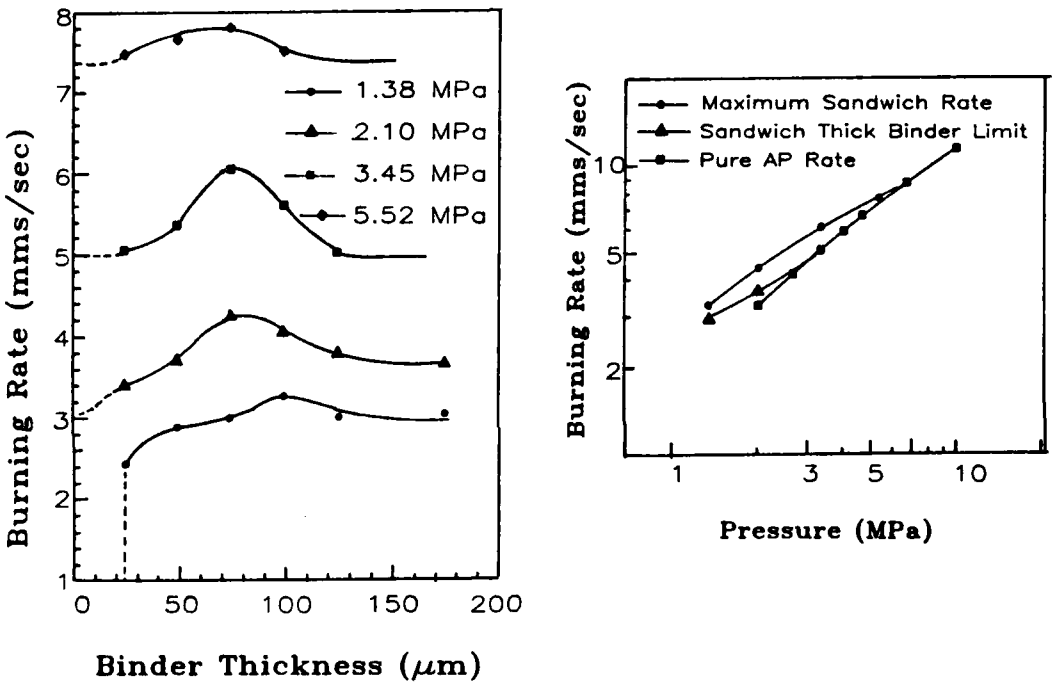

Fig. 5 Burning rate of sandwiches
a) Rate vs binder lamina thickness (data points are experimental measurements)
b) Rate vs pressure (data points are cross-plot points from curves in Fig. 5a)

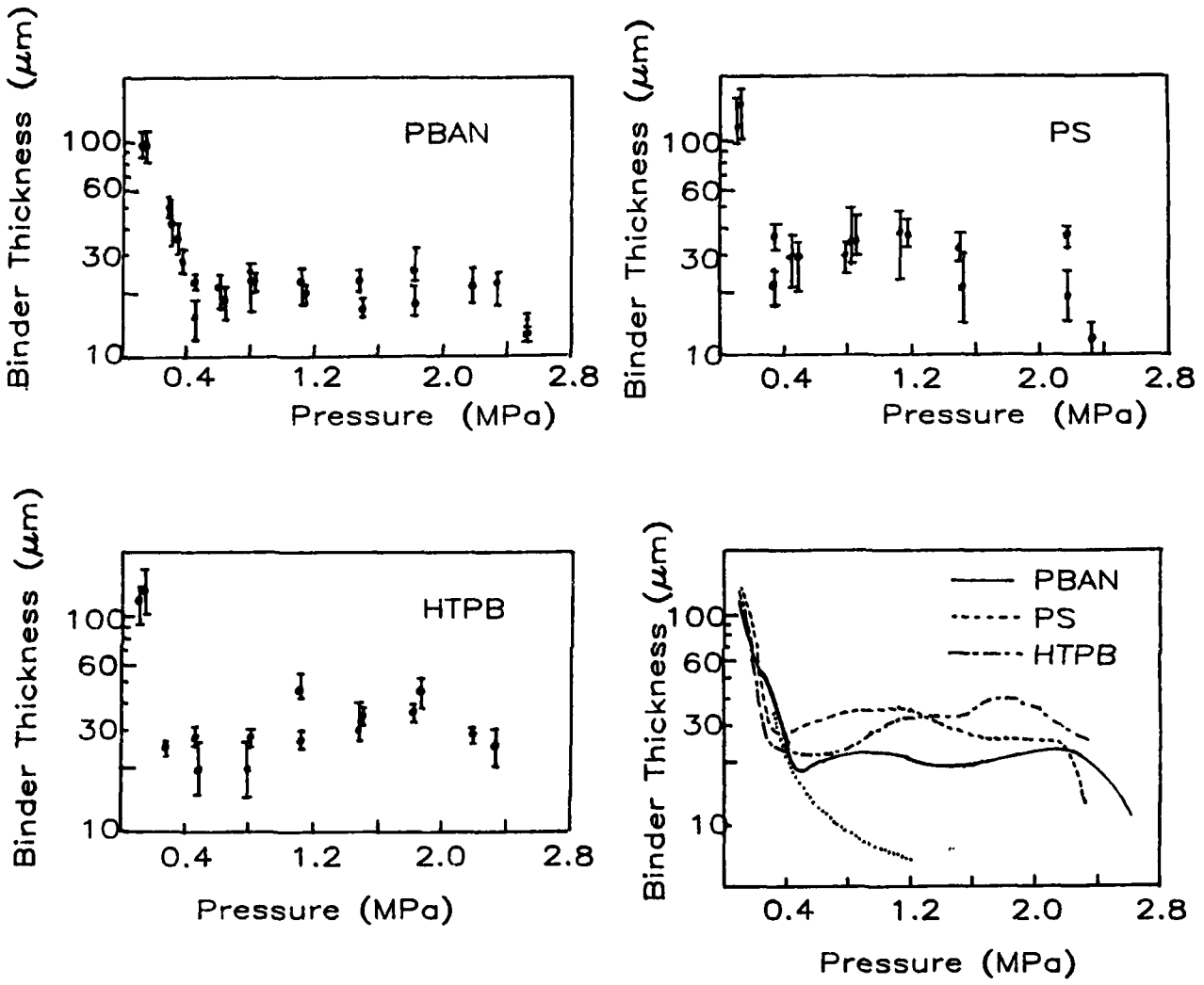

Fig. 6 Spontaneous quench limits for tapered sandwiches burning at constant pressure.

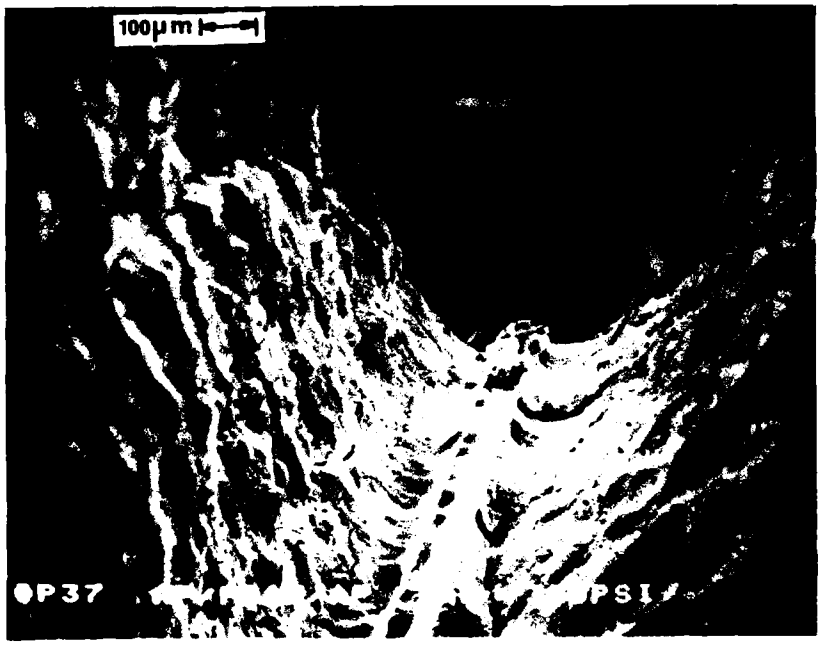

Fig. 7 Surface of a spontaneously quenched sample (test pressure 2.08 MPa).

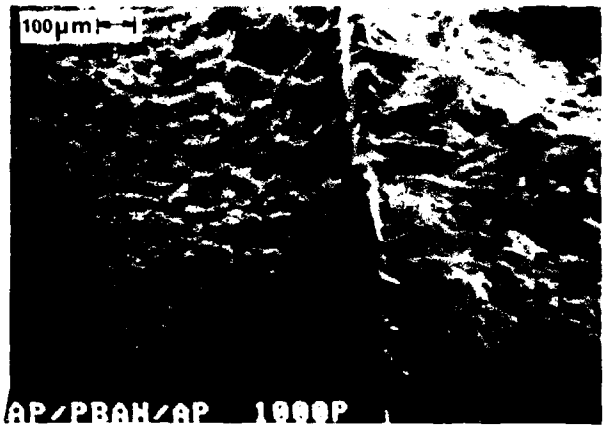

a) Pure PBAN binder lamina

b) 1:1 AP-filled PBAN binder lamina

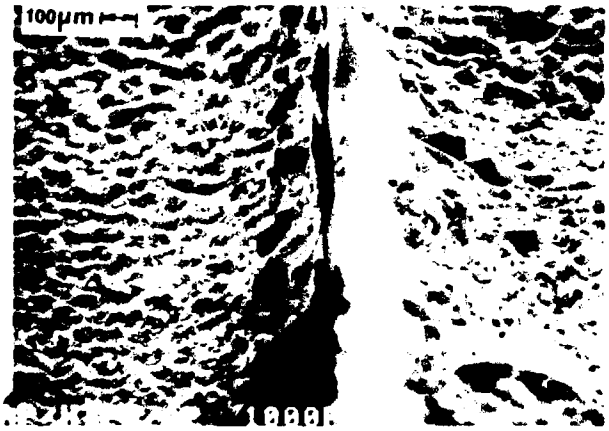

c) Pure HTPB binder lamina

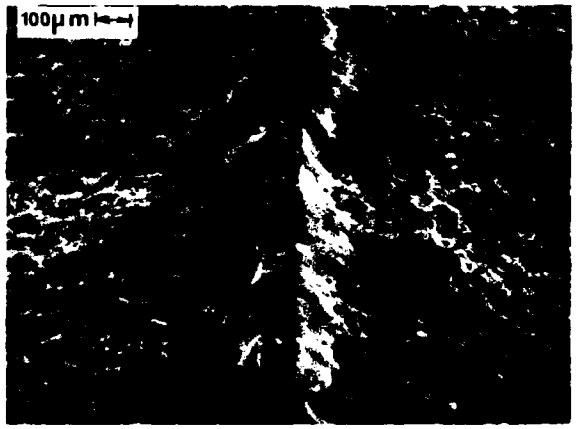

d) 1:1 AP-filled HTPB lamina

Fig. 8 Comparison of quenched surfaces of sandwiches (6.9 MPa)

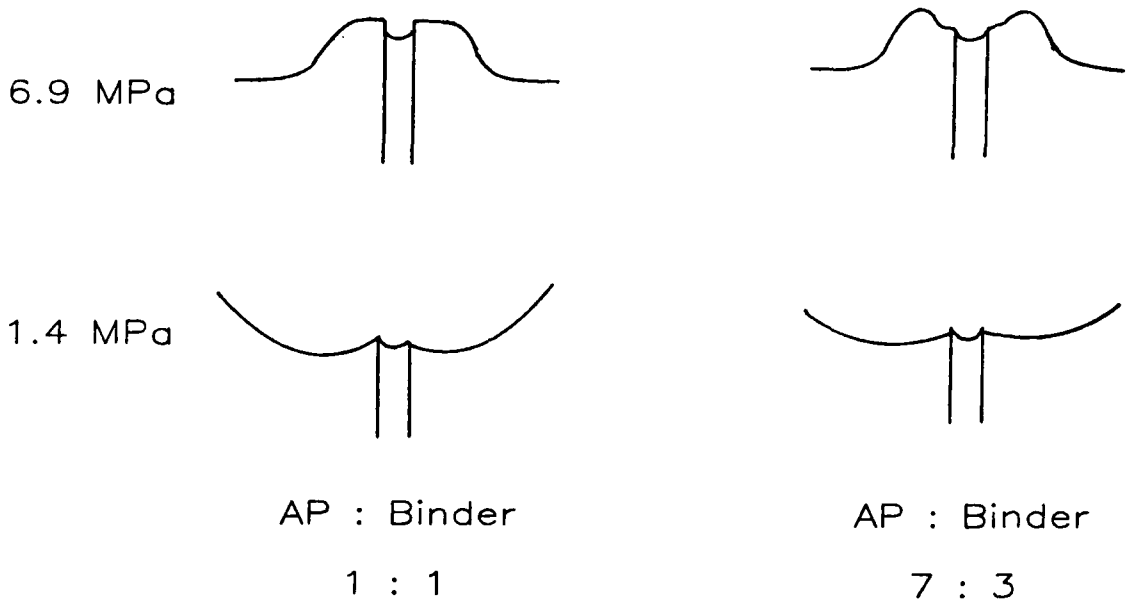

Fig. 9 Surface profiles of sandwiches with different AP-binder ratios in the binder laminae, and different pressures (PBAN binder, lamina thickness approximately 70 μm).

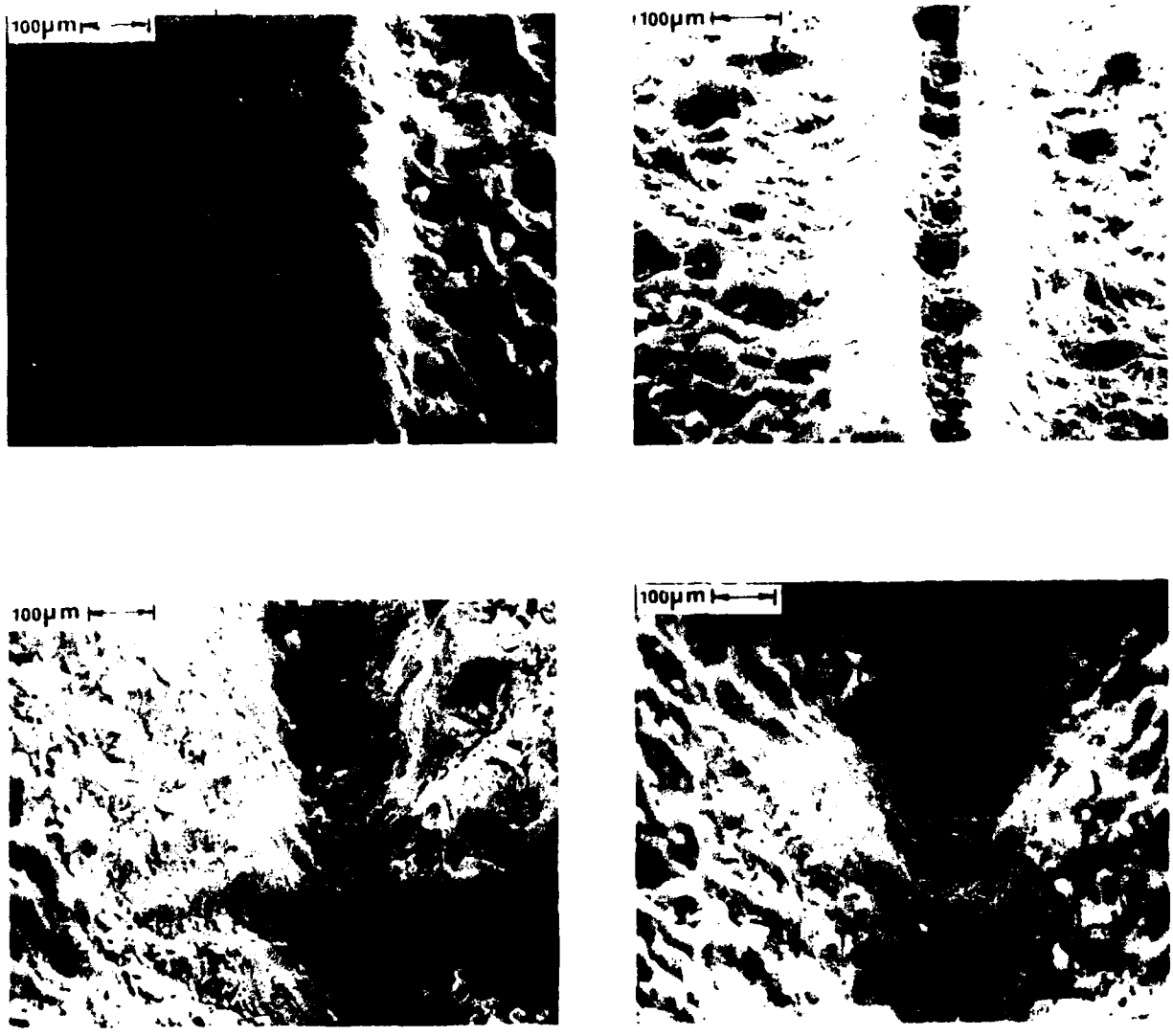

Fig. 10 Effect of lamina thickness on quenched surface with 7:3 AP-filled binder laminae (6.9 MPa).

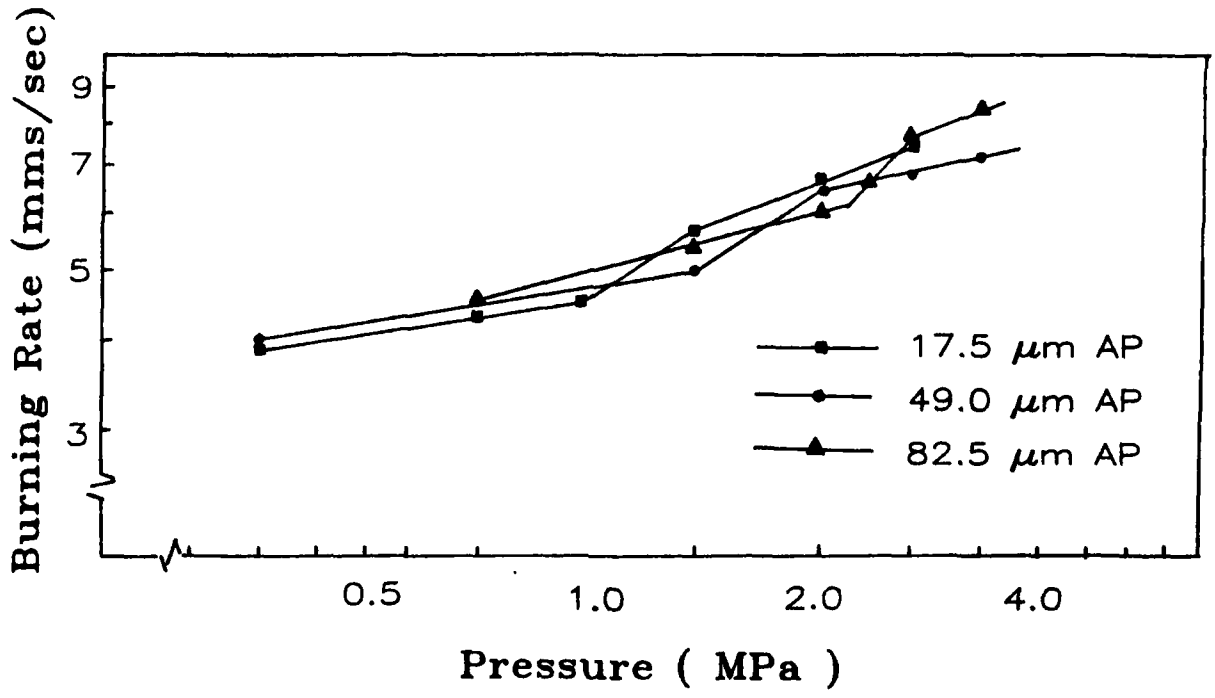

Fig. 11 Burning rate of bimodal propellants.

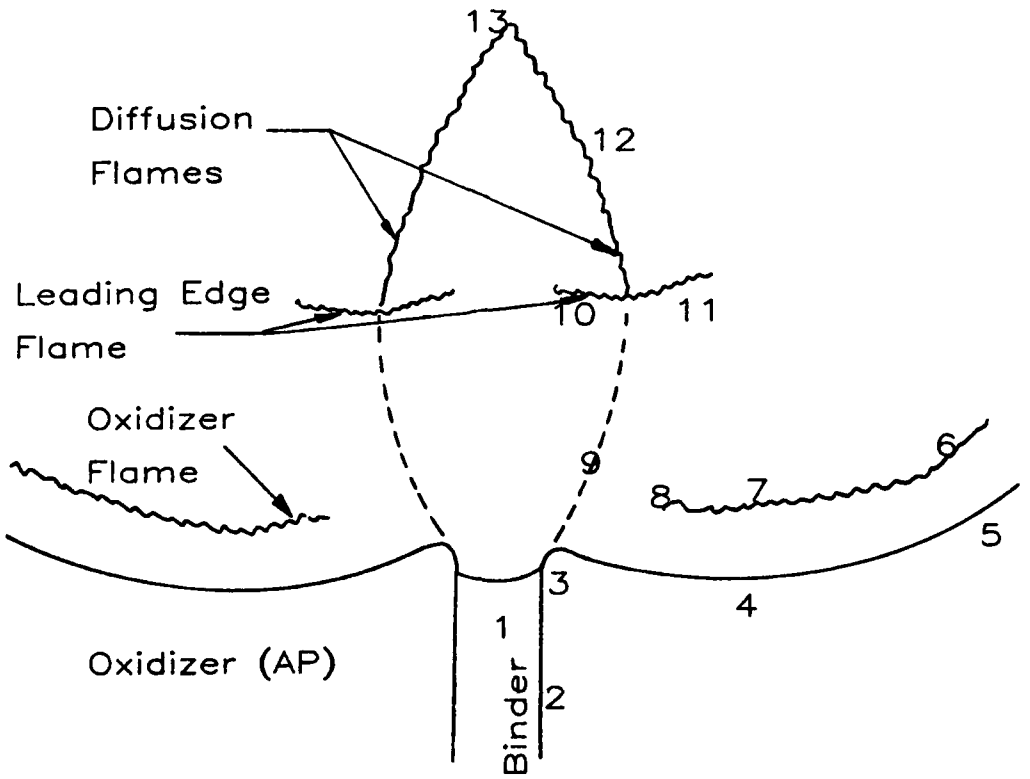

Fig. 12 Principal features of the combustion zone microstructure and processes as suggested by accumulated results. 1. Binder lamina. 2. Interface plane between binder and oxidizer. 3. Oxidizer surface adjoining binder (smooth band). 4. Leading edge of the oxidizer burning front. 5. Oxidizer region that regresses at the normal AP self-deflagration rate. 6. AP flame. 7. Leading edge region of AP flame. 8. Oxidizer flame, modified by the anomalous decomposition in the smooth band (flame may be quenched). 9. Oxidizer-fuel diffusion region, with stoichiometric surface indicated by broken line. 10.-11. Kinetically limited leading edge flame (KLLEF) (fuel-rich and oxidizer-rich sides). 12. Diffusion flame. 13. Tip of diffusion flame.

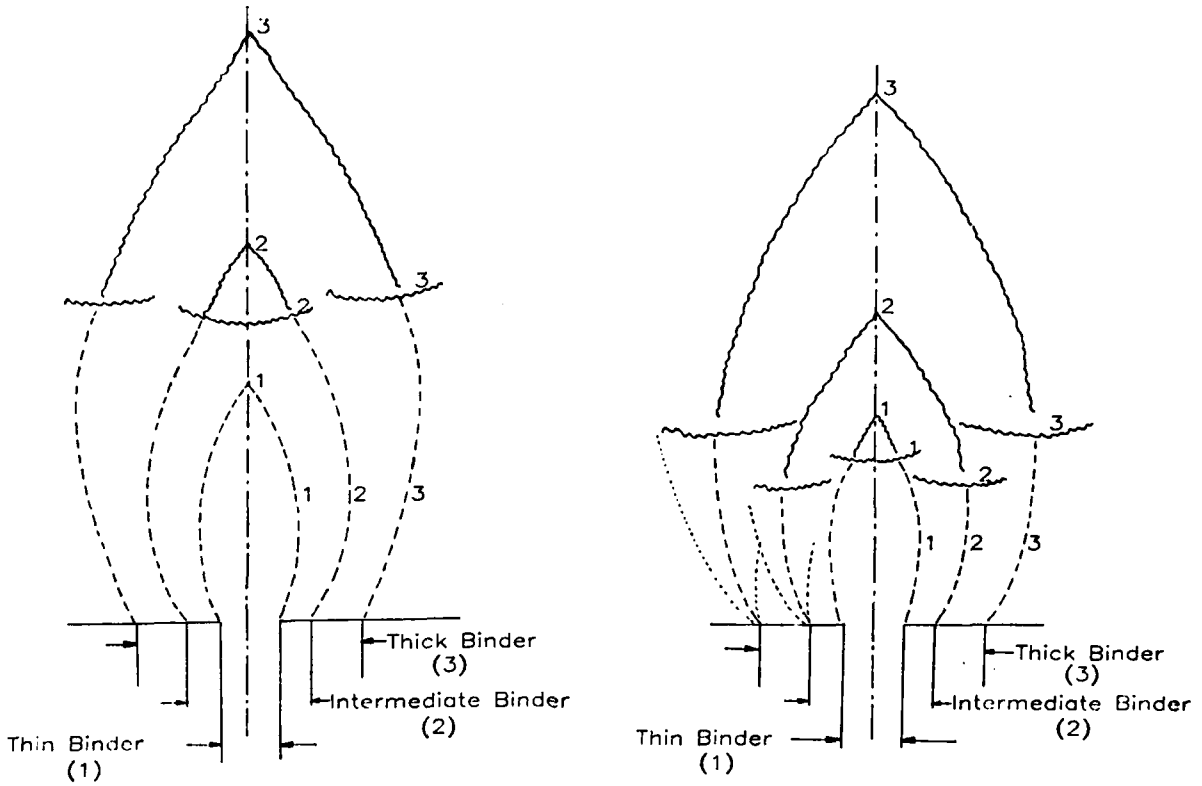

Fig. 13 Trend in surface and oxidizer-binder combustion zone structure with thickness of the binder lamina (flames for different binder thicknesses superimposed)..

a) Very low pressure ($p < 0.4$ MPa) (stoichiometric tip is retracted for binder thickness #1)

b) Low pressure ($0.4 < p < 2.0$ MPa)

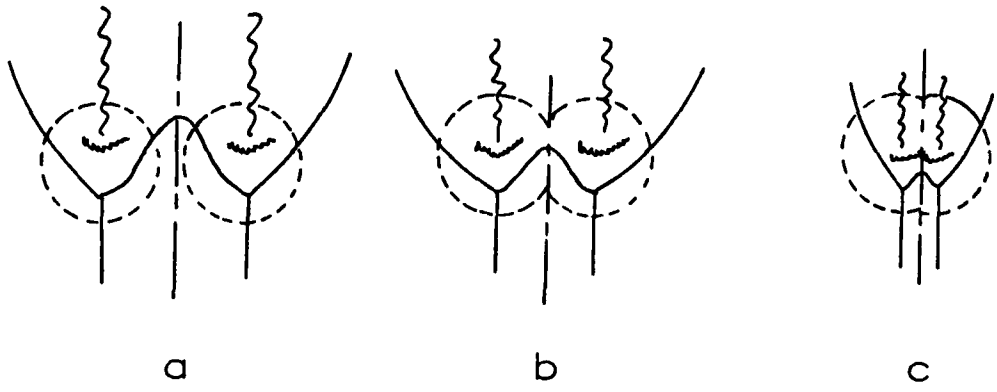

Fig. 14 Propagation velocity controlling regions.
a) Thick binder lamina
b) Binder lamina 70-100 μm
c) Binder lamina $\sim$ 50 μm

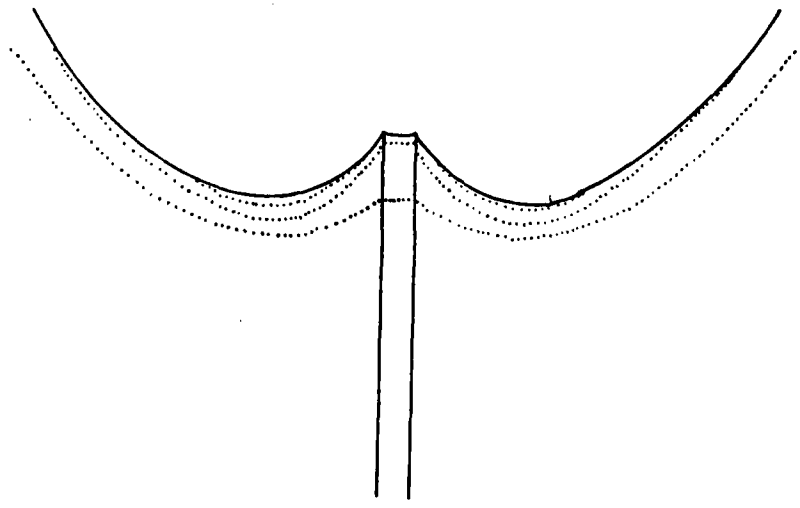

Fig. 15 Temperature field in the solid phase.

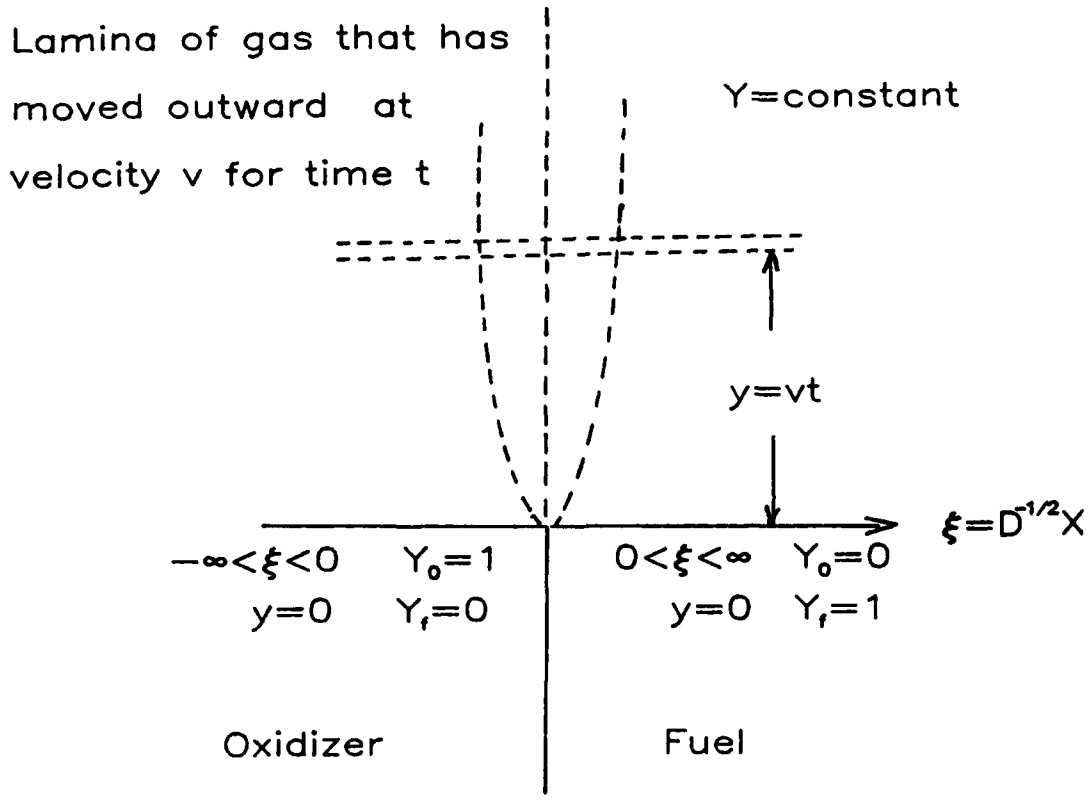

Fig. 16 Description of a single mixing fan.

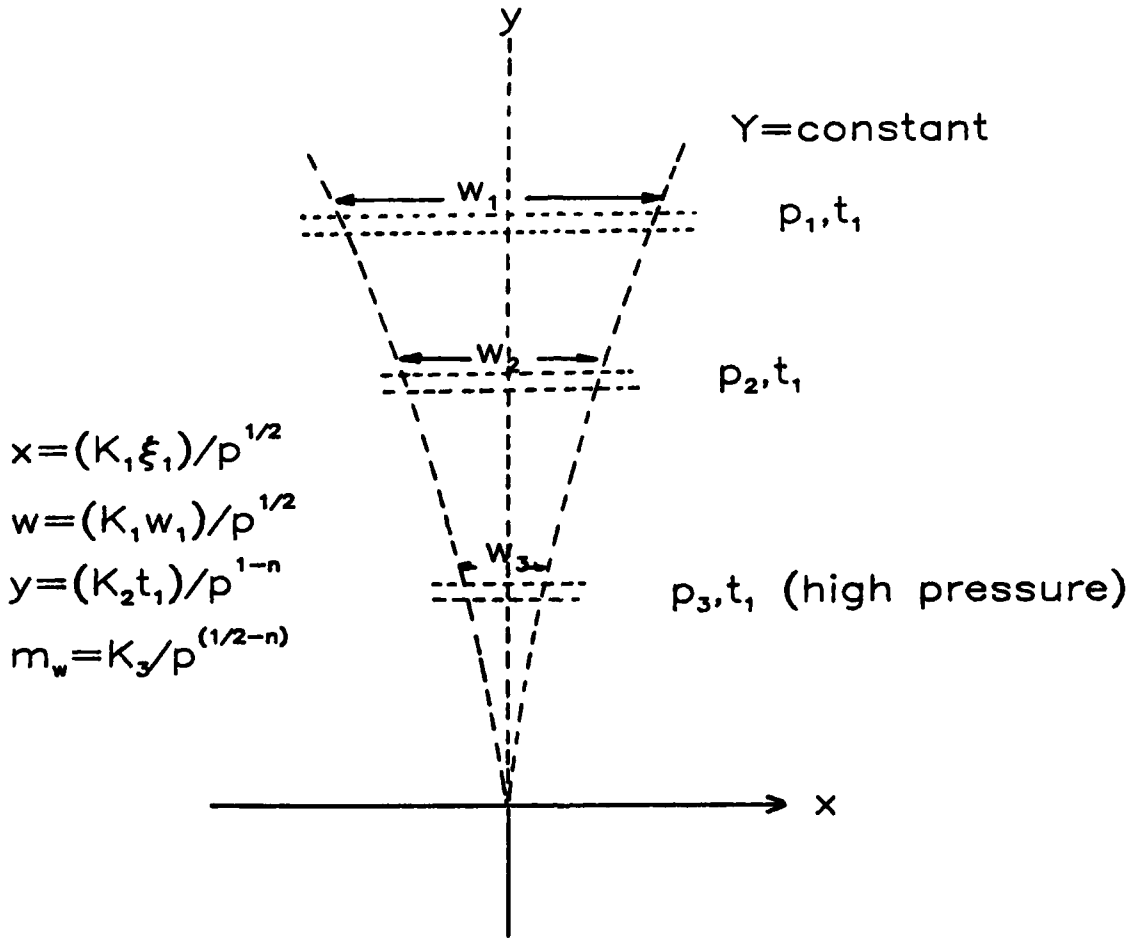

Fig. 17 Dependence of the location and span of the layer vt of the mixing fan on pressure.

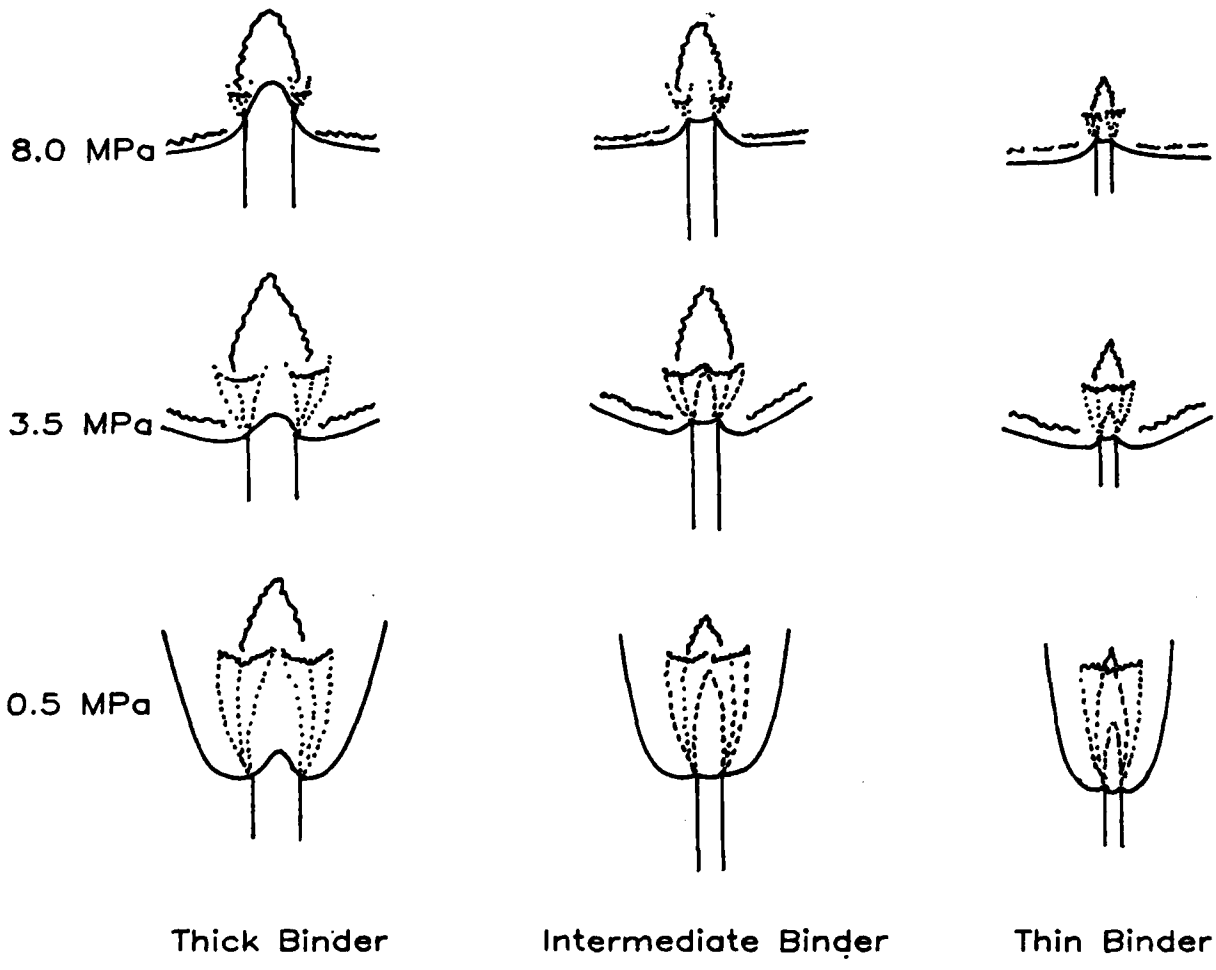

Fig. 18 Dependence of flame complex on pressure for various binder thicknesses (dotted curves are constant-concentration profiles, wavy lines are flames, solid lines are surfaces).

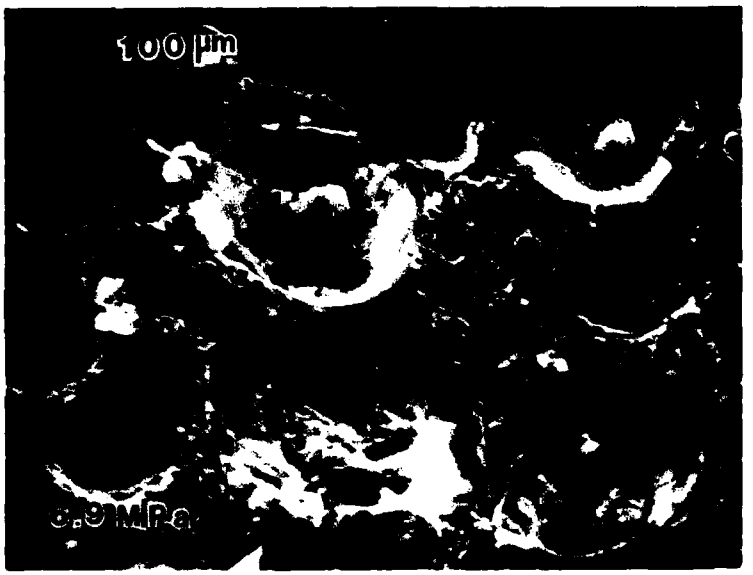

(a)

(b)

Fig. 19 Burned surface of propellant quenched at (a) high and (b) low pressure, illustrating the similarity of surface details with those of sandwiches (AP-PBAN propellant).

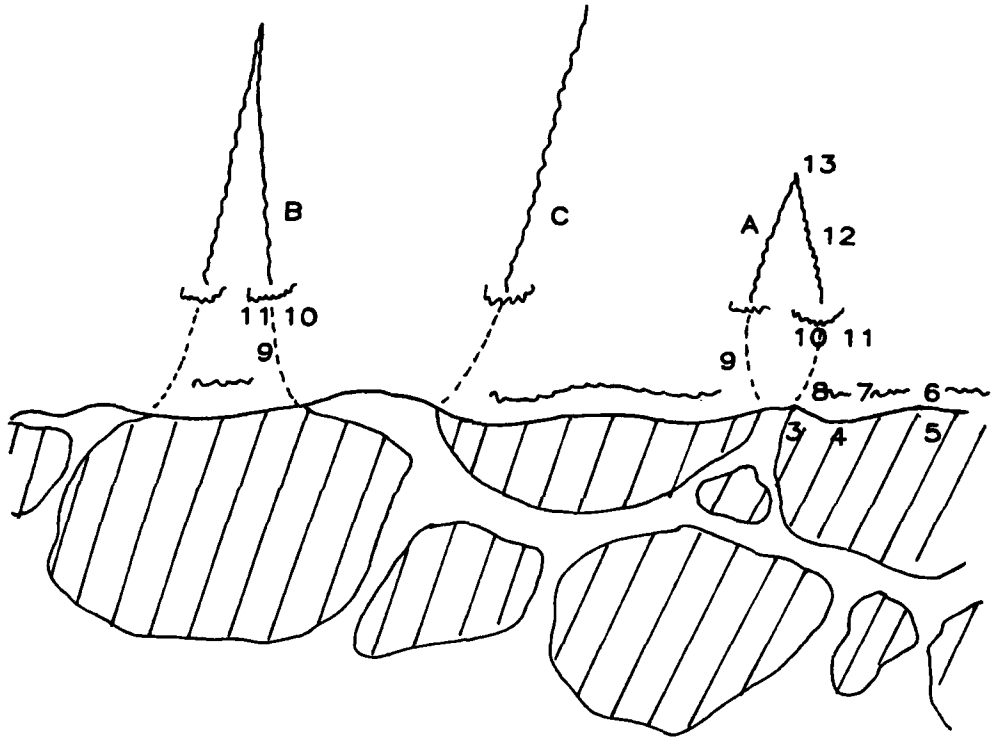

Fig. 20 Combustion zone structure of a propellant such as in Fig. 19, based on analogy with Fig. 12 and 18.

DISTRIBUTION LIST

	No. Copies
Assistant Secretary of the Navy (R, E, and S) Room 5E 731 Pentagon Washington, DC 20350 Attn: Dr. L. V. Schmidt	1
Scientific Advisor Commandant of the Marine Corps Code RD-1 Washington, DC 20380 Attn: Dr. A. L. Slafkosky	1
Office of Naval Research Mechanics Division Code 432 Arlington, VA 22217 Attn: Dr. A. D. Wood	1
Office of Naval Research Mechanics Division Code 432 Arlington, VA 22217 Attn: Dr. Richard S. Miller	10
Office of Naval Research Code 260 Arlington, VA 22217 Attn: Mr. David Siegel	1
Office of Naval Research Western Office 1030 East Green Street Pasadena, CA 91106 Attn: Dr. R. J. Marcus	1
Office of Naval Research East Central Regional Office 666 Summer Street, Bldg. 114-D Boston, MA 02210 Attn: Dr. Larry Peebles	1
Office of Naval Research San Francisco Area Office One Hallidie Plaza, Suite 601 San Francisco, CA 94102 Attn: Dr. Phillip A. Miller	1
Aerojet Solid Propulsion Company P. O. Box 13400, Bldg. 2019/Dept. 4350 Sacramento, CA 95813 Attn: Mr. Michael J. Ditore	1
Aerojet Strategic Propulsion Co. P. O. Box 15699C Sacramento, CA 95813 Attn: Dr. R. L. Lou	1
Aerospace Corporation P. O. Box 92957 Los Angeles, CA 90045 Attn: Ellis M. Landsbaum	1
U. S. Air Force Academy FJSRL/NC USAF Academy, CO 80840 Attn: Dr. John S. Wilkes, Jr.	1
AFATL Code DLDL Eglin AFB, FL 32542 Attn: Mr. Otto K. Heiney	1
Air Force Office of Scientific Research Directorate of Aerospace Sciences Bolling Air Force Base Washington, DC 20332 Attn: Dr. L. H. Caveny	1
Air Force Office of Scientific Research Directorate of Chemical Sciences Bolling Air Force Base Washington, DC 20332 Attn: Mr. Donald L. Ball	1
AFRPL Code PACC Edwards AFB, CA 93523 Attn: Mr. Wayne Roe Mr. J. Levine	2
AFRPL Code MKP/MS24 Edwards AFB, CA 93523 Attn: Mr. R. Geisler	1
AFRPL Code CA Edwards AFB, CA 93523 Attn: Dr. R. R. Weiss	1
Anal-Syn Lab Inc. P. O. Box 547 Paoli, PA 19301 Attn: Dr. V. J. Keenan	1
Army Ballistic Missile Defense Command BMDSC/HEDS P. O. Box 1500 Redstone Arsenal, AL 35807 Attn: Ms. R. Buckalew	1
Army Ballistic Research Labs ARRADCOM Code DRDAR-BLI Aberdeen Proving Ground, MD 21005 Attn: Mr. J. M. Frankle Dr. Ingo W. May Mr. L. A. Watermeier	3
Army Ballistic Research Labs ARRADCOM Code DRDAR-BLP Aberdeen Proving Ground, MD 21005 Attn: Dr. A. W. Barrows	1
HQ US Army Material Development Readiness Command Code DRCDE-DW 5011 Eisenhower Avenue Room 8N42 Alexandria, VA 22333 Attn: Mr. S. R. Matos	1
Army Missile Command Code DRSMI-R Redstone Arsenal, AL 35898 Attn: Dr. R. G. Rhoades	1
Army Missile Command Code DRSMI-RKL Redstone Arsenal, Al 35898 Attn: Dr. W. W. Wharton	1
Army Research & Development Command ARRADCOM Code LCWSL Dover, NJ 07802	1
Army Research & Development Command ARRADCOM Code DRDAR-SCA-PE Dover, NJ 07802 Attn: Mr. L. Stiefel	1
U. S. Army Research Office Chemical & Biological Sciences Div. P. O. Box 12211 Research Triangle Park, NC 27709	1
Atlantic Research Corp. 4390 Cherokee Ave. Alexandria, VA 22314 Attn: Dr. C. B. Henderson Dr. Merill K. King	2
Atlantic Research Corp Pine Ridge Plant 7511 Wellington Rd. Gainesville, VA 22065 Attn: Mr. R. H. W. Waesche	1
Brigham Young University Provo, UT 84601 Attn: Dr. Merrill W. Beckstead	1
British Embassy Munitions Directorate Propellants and Explosives Defence Equipment Staff 3100 Massachusetts Ave. Washington, DC 20008 Attn: Dr. T. Sinden	1
California Institute of Tech. Graduate Aeronautical Lab Pasadena, CA 91125 Attn: Prof. W. G. Knauss	1
California Institute of Tech. Dept. of Chemical Engineering Pasadena, CA 91125 Attn: Prof. N. W. Tschoegl	1
California Institute of Tech. 204 Karman Lab 1201 E. California St. Pasadena, CA 91109 Attn: Fred E. C. Culick	1

DISTRIBUTION LIST

	No. Copies
California Institute of Tech. Jet Propulsion Laboratory 4800 Oak Grove Drive Pasadena, CA 91103 Attn: Leon D. Strand	1
Calspan Corporation P. O. Box 235 Buffalo, NY 14221 Attn: Edward B. Fisher	1
Catholic Univ. of America Physics Department 520 Michigan Ave., NE Washington, DC 20017 Attn: Prof. T. Litovitz	1
Mr. Norman Cohen 141 Channing Street Redlands, CA 92373	1
Defense Technical Information Center Code DTIC-DDA-2 Cameron Station Alexandria, VA 22314	12
General Dynamics Pomona Division Mail Zone 4-87 P. O. Box 2507 Pomona, CA 91769 Attn: Mr. D. E. Taylor	1
Georgia Institute of Tech. School of Aerospace Engineering Atlanta, GA 30332 Attn: Prof. Edward Price	1
Hercules Inc. Aerospace Division Alleghany Ballistic Lab P. O. Box 210 Cumberland, MD 21502 Attn: Dr. Rocco C. Musso Dr. R. R. Miller	2
Hercules Inc. Bacchus Works P. O. Box 98 Magna, UT 84044 Attn: Dr. E. H. Debutts Dr. James H. Thacher Dr. K. McCarty	3
Hercules Inc. Eglin Code AFATL/DLDL Eglin AFB, FL 32542 Attn: Dr. Ronald L. Simmons	1
Hercules, Inc. P. O. Box 548 McGregor, TX 76657 Attn: Mr. William G. Haymes	1
IBM Research Lab D42.282 San Jose, CA 95193 Attn: Dr. Thor L. Smith	1
Institute for Defense Analyses 1801 N. Beauregard Street Alexandria, VA 22311 Attn: Mr. R. C. Oliver	1
Johns Hopkins University APL Chemical Propulsion Info. Agency Johns Hopkins Road Laurel, MD 20810 Attn: Mr. Thomas W. Christian Mr. Theodore M. Gilliland	2
Lawrence Livermore Laboratory University of California Code L-324 Livermore, CA 94550 Attn: Dr. R. McGuire	1
Lockheed Missile & Space Co. Code 83-10, Bldg. 154 P. O. Box 504 Sunnyvale, CA 94088 Attn: Dr. Jack Linsk	1
Lockheed Missile & Space Co. Dept. 52-35, Bldg. 204/2 3251 Hanover Street Palo Alto, CA 94304 Attn: Dr. H. P. Marshall	1
Los Alamos Scientific Lab Mail Stop 920 Los Alamos, NM 87545 Attn: Ms. Joan L. Janney	1
Los Alamos Scientific Lab Code WX-2, MS-952 P. O. Box 1663 Los Alamos, NM 87545 Attn: Dr. R. L. Rabie	1
Los Alamos Scientific Lab Code WX-2 P. O. Box 1663 Los Alamos, NM 87545 Attn: Dr. R. Rogers	1
Los Alamos Scientific Lab P. O. Box 1663 Los Alamos, NM 87545 Attn: Dr. J. M. Walsh	1
Morton Thiokol Corp. Elkton Division P. O. Box 241 Elkton, MD 21921 Attn: Mr. W. Brundige	1
Morton Thiokol Corp. Government Systems Group Technical Director P. O. Box 9258 Ogden, Utah 84409 Attn: Dr. T. F. Davidson	1
Morton Thiokol Corp. Huntsville Division Huntsville, AL 35807 Attn: Mr. R. Wall Mr. R. B. Kruse	2
Morton Thiokol Corp. Wasatch Division P. O. Box 524 Brigham City, UT 84302 Attn: Dr. J. C. Hinshaw Mr. John A. Peterson Dr. G. Thompson	3
NASA/George C. Marshall Space Flight Center Code EP 25 Huntsville, AL 35812 Attn: J. Q. Miller	1
NASA/George C. Marshall Space Flight Center Code EP 24 Huntsville, AL 35812 Attn: Robert J. Richmond	1
NASA/HQ Code RP 600 Independence Ave., SW, Rm. 625 Washington, DC 20546 Attn: Frank W. Stephenson, Jr.	1
Naval Air Systems Command Code AIR-310 F Washington, DC 20361 Attn: Mr. E. A. Lichtman	1
Naval Air Systems Command Code AIR-310C Washington, DC 20360 Attn: Dr. H. Rosenwasser	1
Naval Air Systems Command Code 03P25 Washington, DC 20360 Attn: Mr. B. Sobers	1
Naval Air Systems Command Code NAIR-954-Tech Library Washington, DC 20361	1
Naval Explosives Dev. Engineering Department Assistant Director Naval Weapons Station Yorktown, VA 23691 Attn: Dr. L. R. Rothstein	1
Naval Explosive Ordnance Disposal Tech Center Code D Indian Head, MD 20640 Attn: Dr. Lionel Dickinson	1

DISTRIBUTION LIST

	No. Copies
Naval Materiel Command Strategic Systems Project Office Propulsion Unit Code SP 2731 Department of the Navy Washington, DC 20376	1
Naval Materiel Command Strategic Systems Project Office Department of the Navy Room 1048 Washington, DC 20376 Attn: Mr. E. L. Throckmorton	1
Naval Ocean Systems Center San Diego, CA 92152 Attn: Mr. Joe McCartney	1
Naval Ocean Systems Center Marine Sciences Division San Diego, CA 91232 Attn: Dr. S. Yamamoto	1
Naval Ordnance Station PM4 Indian Head, MD 20640 Attn: Mr. C. L. Adams	1
Naval Ordnance Station Code 5253 Indian Head, MD 20640 Attn: Mr. S. Mitchell	1
Naval Ordnance Station Indian Head, MD 20640 Attn: Mr. Peter L. Stang	1
Naval Postgraduate School Dean of Research Monterey, CA 93940 Attn: Dr. William Tolles	1
Naval Postgraduate School Physics & Chemistry Dept. Monterey, CA 93940 Attn: Prof. Richard A. Reinhardt	1
Naval Postgraduate School Department of Aeronautics Monterey, CA 93940 Attn: Mr. David W. Netzer	1

	No. Copies
Naval Research Lab. Code 4040 Washington, DC 20375 Attn: Dr. Elaine Oran	1
Naval Research Lab. Code 6100 Washington, DC 20375	1
Naval Research Lab. Code 6510 Washington, DC 20375 Attn: Dr. J. Schnur	1
Naval Sea Systems Command Code SEA 64E Washington, DC 20362 Attn: Mr. R. Beauregard	1
Naval Sea Systems Command Code 62R3 Washington, DC 20362 Attn: Mr. G. Edwards	1
Naval Sea Systems Command NAV SEA 62R22 Crystal Plaza, Bldg. 6, Rm 806 Washington, DC 20362 Attn: Mr. Robert F. Cassel	1
Naval Sea Systems Command Code 62R2 Washington, DC 20362 Attn: Mr. C. M. Christensen	1
Naval Ship Engineering Center Materials Branch Philadelphia, PA 19112 Attn: Mr. John Boyle	1
Naval Ship Research & Development Center Applied Chemistry Division Annapolis, MD 21401 Attn: Dr. G. Bosmajian	1
Naval Surface Weapons Center Commander Silver Spring, MD 20910 Attn: Mr. G. B. Wilmot	4

	No. Copies
Naval Surface Weapons Center Code RO4 White Oak Laboratory Silver Spring, MD 20910 Attn: Dr. D. J. Pastine	1
Naval Surface Weapons Center Code R10 White Oak Laboratory Silver Spring, MD 20910 Attn: Dr. S. J. Jacobs	1
Naval Surface Weapons Center Code R11 White Oak Laboratory Silver Spring, MD 20910 Attn: Dr. H. G. Adolph Dr. T. Hall Dr. M. J. Kamlet Dr. K. F. Mueller	4
Naval Surface Weapons Center Code R13 White Oak Laboratory Silver Spring, MD 20910 Attn: Dr. E. Zimmet Dr. R. Bernecker	2
Naval Surface Weapons Center Code R16 Indian Head, MD 20640 Attn: Dr. T. D. Austin	1
Naval Surface Weapons Center Code R101 Indian Head, MD 20640 Attn: Mr. G. L. Mackenzie	1
Naval Surface Weapons Center Code R121 White Oak Laboratory Silver Spring, MD 20910 Attn: Mr. M. Stosz	1
Naval Surface Weapons Center Code R122 White Oak Laboratory Silver Spring, MD 20910 Attn: Mr. L. Roslund	1

	No. Copies
Office of Naval Technology Chief MAT Code 0716 Washington, DC 20360 Attn: Dr. A. Faulstich	1
Office of Naval Technology Chief of Naval Material MAT Code 0712 Washington, DC 20360 Attn: LCDR J. Walker	1
Naval Underwater Systems Center Energy Conversion Dept. Code 5B331 Newport, RI 02840 Attn: Mr. Robert S. Lazar	1
Naval Weapons Center Code 385 China Lake, CA 93555 Attn: Dr. A. Amster Dr. A. Nielsen	2
Naval Weapons Center Code 389 China Lake, CA 93555 Attn: Mr. T. L. Boggs Dr. R. L. Derr Dr. R. Reed, Jr.	3
Naval Weapons Center Code 3205 China Lake, CA 93555 Attn: Mr. Lee N. Gilbert Dr. L. Smith Dr. C. Thelen	3
Naval Weapons Center Code 3272 China Lake, CA 93555 Attn: Mr. R. McCarten	1
Naval Weapons Center Code 3858 China Lake, CA 93555 Attn: Dr. E. Martin	1

DISTRIBUTION LIST

	No. Copies
Naval Weapons Support Center Code 5042 Crane, IN 47522 Attn: Dr. B. Douda	1
Northwestern University Dept. of Civil Engineering Evanston, IL 60201 Attn: Prof. J. D. Achenbach	1
Pennsylvania State University Dept. of Mechanical Engineering University Park, PA 16802 Attn: Prof. Kenneth Kuo	1
Princeton Combustion Research Laboratories, Inc. 1041 U. S. Highway One North Princeton, NJ 08540 Attn: Dr. Martin Summerfield Dr. J. Ben Raven	2
Princeton University School of Engineering and Applied Sciences Dept. of Mech. Eng. & Aero. Eng. The Engineering Quadrangle Princeton, NJ 08544 Attn: Dr. Forman A. Williams	1
Purdue University School of Mechanical Engineering TSPC Chaffee Hall West Lafayette, IN 47906 Attn: Mr. John R. Osborn	1
Rockwell International Corp. Rocketdyne Division BA08 6633 Canoga Ave. Canoga Park, CA 91304 Attn: Mr. Joseph E. Flanagan	1
Rohm and Haas Company Huntsville, AL 35801 Attn: Dr. H. Shuey Mr. W. Stone	2
Sandia Laboratories Division 2513 P. O. Box 5800 Albuquerque, NM 87185 Attn: Dr. S. Sheffield	1
Space Sciences, Inc. 135 Maple Avenue Monrovia, CA 91016 Attn: Dr. M. Farber	1
Southwest Research Institute Institute Scientist P. O. Drawer 28510 San Antonio, TX 78228 Attn: Mr. William H. McLain	1
Texas A & M University Dept. of Civil Engineering College Station, TX 77843 Attn: Prof. Richard A. Schapery	1
United Technologies Corp. Chemical Systems Division P. O. Box 358 Sunnyvale, CA 94088 Attn: Dr. Robert S. Brown Dr. C. M. Frey Dr. R. W. Hermsen	3
University of Akron Institute of Polymer Science Akron, OH 44325 Attn: Prof. Alan N. Gent	1
University of California Berkeley, CA 94720 Attn: Prof. A. G. Evans	1
University of California Dept. of Chemistry 405 Hilgard Ave. Los Angeles, CA 90024 Attn: Prof. M. D. Nicol	1
University of Delaware Department of Chemistry Newark, DE 19711 Attn: Dr. T. C. Brill	1
University of Illinois AE Dept. Transportation Building, Room 105 Urbana, IL 61801 Attn: Dr. Herman Krier	1
University of Maryland Dept. of Mechanical Engineering College Park, MD 20742 Attn: Prof. R. W. Armstrong	1
University of Southern California Mechanical Engineering Dept. OHE 200 Los Angeles, CA 90007 Attn. Dr. M. Gerstein	1
University of Utah Salt Lake City, UT 84112 Attn: Dr. G. A. Flandro	1
University of Utah Dept. of Mech. & Ind. Eng. MEB 3008 Salt Lake City, UT 84112 Attn: Dr. Stephen Swanson	1
University of Waterloo Dept. of Mechanical Engineering Waterloo, Ontario CANADA Attn: Dr. Clarke E. Hermance	1
Washington State University Dept. of Physics Pullman, WA 99163 Attn: Prof. G. D. Duvall Prof. T. Dickinson	2
Whittaker Corporation Bermite Division 22116 W. Soledad Canyon Road Saugus, CA 90024 Attn: Mr. L. Bloom	1